

**Development of Surface Pretreatments
of Aluminum Alloy EN AW-6061 for
Metal-Polymer Hybrid Joints**



By

Usama Naeem

School of Chemical and Materials Engineering

National University of Science and Technology

2022

Development of Surface Pretreatment of Aluminum Alloy EN AW-6061 for Metal-Polymer Hybrid Joints



Name: Usama Naeem

Reg No: 00000275011

**This thesis is submitted as a partial fulfillment of the requirements for
the degree of**

MS (Materials and Surface & Engineering)

Supervisor Name: Dr. Mohsin Saleem

School of Chemical and Materials Engineering (SCME)

National University of Sciences and Technology (NUST)

H-12 Islamabad, Pakistan

August, 2022

DEDICATION

I dedicate this thesis to my loving Parents, caring wife, and son, who loved me always unconditionally and their support inspired me for hardworking and struggle for the things that I aspire to achieve. I am extremely grateful to all my friends and lab mates for their kind support and guidance.

Acknowledgements

All the praises to Almighty Allah, who's mercy is endless and who has given me ability and courage to complete my degree, and salat to His messenger Muhammad (PBUH), under whose guidance I am moving towards my lighthouse.

I am appreciative to my supervisor **Dr. Mohsin Saleem**, under whose expertise I accomplished this research. His agility of mind and clarity of ideas put my research on track. His kindness and support beyond expression and words fall deficient to express my appreciation. I believe that without his constant and brilliant supervision I could not complete my research.

I pay my special thanks to **Dr. Muhammad Irfan** his cool and humble behavior motivated me to perform my best and giving expert views and suggestions to make my study more productive, his special interest in my research and giving me best piece of advice and encouragement at every step of research.

I am also thankful to my guidance committee members **Dr. Sofia Javed** and **Dr. Asma Hayat (GCU Lahore)** for their help in my work.

I am thankful to the Principal of SCME **Dr. Amir Azam Khan** who allowed me to pursue my research in this field. I express my gratitude to the head of the Materials Engineering department **Dr. Khurram Yaqoob**, and PG coordinator **Dr. Usman Liaqat**, for providing a positive research environment and allowing me all required facilities in department and helping and motivating me through out in my research.

I would like to acknowledge all the faculty members and supporting staff at SCME for being cooperative. and supportive I also pay my special thanks to my friends Hamza Rafiq, Munawar Ali, Muhammad Fasih, Sajjad Ahmed, Abdul Waheed, Abdul Rafay, Farhan Raheel, Lab Eng. M. Zafar, Khawer Bhai, Ajmal Hameed, M Faraz, Ali Haider, Asad Malik and Ehtisham Nasir for their help and guidance at different stages of my research.

Finally, to all my family specially my mother, wife, and son for their kind prayers and their support.

Abstract

Surface pretreatments of aluminum alloys are known to be of great importance for stronger and environmentally stable adhesively bonded joints. Aluminum alloy adhesive joints offer a wide range of potential applications in the automotive and aerospace industries, thus detailed research of their performance is necessary. Better surface treatment of the substrates is necessary to offer good surface characteristics that will increase the strength and stability of adhesive joints. In this work surface pretreatments like degreasing, grit blasting, and/or anodizing are done on aluminum alloy EN-AW-6061. Surface roughness profile was studied through optical profilometry. Surface morphological studies were done through scanning electron microscopy (SEM) and compositional analysis through energy dispersive X-ray spectroscopy (EDX). The surface pretreated substrates were adhesively bonded using polyamide or nylon-6 (PA-6) in a convection oven. The bond line thickness was measured using optical microscopy. Single lap shear testing of adhesively bonded joints was performed at tensile testing machine. The grit blasted samples showed a good roughness value Ra of around 14 μm and 15 μm as compared to the degreased ones which showed Ra of 0.5 μm . The grit blasted and anodized samples showed good lap shear strengths of 19 MPa and 16 MPa, respectively. The control samples, i.e., as received, or degreased ones demonstrated a very low lap shear strength of 9 MPa and 13 MPa, respectively. After hydrothermal aging, the lap shear strengths of grit blasted samples were dropped to a 5 MPa, whereas the samples received other pretreatments showed almost zero lap shear strengths after this hydrothermal treatment. The fracture analysis revealed the polymer residues on grit blasted surfaces of and no such residues were observed at fracture surfaces of decrease or as received samples. This observation explained the better performance of decreased samples compared to that of as received or degreased ones.

Table of Contents

Chapter:1.....	1
Introduction	1
1.1 Need for adhesive joining	1
1.2 Surface pretreatment role in adhesive joining	1
1.3 Aluminum and its alloys	2
1.3.1 Aluminum.....	2
1.3.2 Aluminum alloys.....	3
1.4 Surface pretreatments	3
1.4.1 Degreasing (DG)	4
1.4.2 Grit Blasting.....	5
1.4.3 Phosphoric acid anodizing (PAA).....	5
1.5 Aims & objective	6
Chapter:2.....	7
Literature Review	7
Chapter:3.....	10
Experimental Procedure	10
3.1 Materials	10
3.1.1. Dimensions of Specimen.....	10
3.2. Surface pretreatment.....	12
3.2.1. Degreasing.....	12
3.2.2. Grit Blasting.....	12
3.2.3. Phosphoric acid anodizing (PAA).....	13
3.3. Adhesive Bonding process	14
3.3.1. Design and Fabrication of bonding tool.....	15
3.4. Thermal joining process	22
Chapter:4.....	23
Characterization Techniques.....	23
4.1. Mechanical Testing	23
4.1.1. Single Lap Shear Joint Test.....	23
4.1.2. Hydrothermal Aging.....	24
4.2. Scanning electron microscopy (SEM).....	25

4.3. Energy dispersive x-ray spectroscopy (EDS or EDX).....	26
4.4. Optical Profilometry.....	26
4.5. Optical Microscopy	26
Chapter:5.....	28
Results and Discussion	28
5.1. Morphological study of un bonded pretreated surfaces: Unaged	28
5.1.1. As Received	28
5.1.2. Degreased	28
5.1.3. Grit Blast at 2cm Distance (GB2).....	29
5.1.4. Grit Blast at 8cm Distance (GB8).....	30
5.1.5. Phosphoric acid Anodizing (PAA)	30
5.2. Morphological study of unbonded pretreated surfaces: Aged.....	31
5.2.1. As Received	31
5.2.2. Degreased	32
5.2.3. Grit Blast at 2cm Distance (GB2).....	32
5.2.4. Grit Blast at 8cm Distance (GB8).....	33
5.3. Topographical Analysis.....	33
5.4. Bondline Thickness of adhesively bonded joints	34
5.5. Single lap joint shear strengths.....	35
5.6. Fracture Analysis: unaged samples.....	37
5.6.1. Morphological study	37
5.6.1.1. As Received	37
5.6.1.2. Degreased	38
5.6.1.3. Grit Blast at 2cm Distance (GB2).....	39
5.6.1.4. Grit Blast at 8cm Distance (GB8).....	39
5.6.2. Compositional study	40
5.6.2.1. As Received	40
5.6.2.2. Degreased	42
5.6.2.3. Grit Blasting with 2cm Distance (GB2).....	44
5.6.2.4. Grit Blasting with 8cm Distance (GB8).....	46
5.7. Fracture analysis: aged samples.....	48
5.7.1. Morphological study	48
5.7.1.1. As Received	48

5.7.1.2. Degreased	49
5.7.1.3. Grit Blasting with 2cm Distance (GB2)	50
5.7.1.4. Grit Blasting with 8cm Distance (GB8)	50
5.7.2. Compositional study	51
5.7.2.1. As Received	51
5.7.2.2. Degreased	53
5.7.2.3. Grit Blasting with 2cm Distance (GB2)	55
5.7.2.4. Grit Blasting with 8cm Distance (GB8)	57
Conclusions	60
References.....	61

List of Figures

Figure 3.1- 1 EN AW-6061 T6 Sheet	11
Figure 3.1- 2 Laser Cutting of EN AW-6061 T6 Sheet	11
Figure 3.1- 3 EN AW-6061-T6 Sheet after Laser cutting.....	12
Figure 3.2- 1 Standard PAA pretreatment flow chart	13
Figure 3.2- 2 Phosphoric acid anodizing Setup.....	14
Figure 3.3- 1 Bonding tool for Adhesive Joints	15
Figure 3.3- 2 First design of Bonding tool	16
Figure 3.3- 3 New design of Bonding tool.....	17
Figure 3.3- 4 3D Image of Bonding tool.....	18
Figure 3.3- 5 Manufacturing of Bonding tool by CNC milling machine.....	19
Figure 3.3- 6 Holes dimensions for m3 screw	20
Figure 3.3- 7 M3 screw holes drilling and tapping	21
Figure 4.1- 1 Schematic of substrate for single lap joint shear test	23
Figure 4.1- 2 Single lap joint shear test setup	24
Figure 4.1- 3 Hydrothermal Aging setup	25
Figure 4.5- 1 Sample preparation for Optical Microscope.....	27
Figure 5.1- 1 SEM image of as received sample.....	28
Figure 5.1- 2 SEM image of degreased sample	29
Figure 5.1- 3 SEM image of GB2 sample.....	29
Figure 5.1- 4 SEM image of GB8 sample.....	30
Figure 5.1- 5 SEM image of (PAA) sample.....	31
Figure 5.2- 1 SEM image of as received sample.....	31
Figure 5.2- 2 SEM image of degreased sample	32
Figure 5.2- 3 SEM image of GB2 sample.....	32
Figure 5.2- 4 SEM image of GB8 sample.....	33
Figure 5.3- 1 Surface roughness values Ra, Rq and Rz of diff. surface treatments.....	34
Figure 5.4- 1 Bond line of Sample 1	35
Figure 5.4- 2 Bond line thickness of sample 2.....	35
Figure 5.5- 1 Lap shear strength of Pretreated samples	37
Figure 5.6- 1 Fracture surface of unaged As Received sample.....	38

Figure 5.6- 2 Fracture surface of unaged Degreased sample	38
Figure 5.6- 3 Fracture surface of unaged GB2cm sample.....	39
Figure 5.6- 4 Fracture surface of unaged GB8cm sample.....	40
Figure 5.6- 5 EDS mapping of unaged as received sample	41
Figure 5.6- 6 Elemental composition of unaged as received sample	42
Figure 5.6- 7 EDS mapping of unaged degreased sample	43
Figure 5.6- 8 Elemental composition of unaged degreased sample.....	44
Figure 5.6- 9 EDS mapping of unaged GB2cm sample.....	45
Figure 5.6- 10 Elemental composition of unaged GB2cm sample	46
Figure 5.6- 11 EDS mapping of unaged GB 8cm sample.....	47
Figure 5.6- 12 Elemental composition of unaged GB 8cm sample	48
Figure 5.7- 1 Fracture surface of aged As Received sample.....	49
Figure 5.7- 2 Fracture surface of aged Degreased sample	49
Figure 5.7- 3 Fracture surface of aged GB2cm sample.....	50
Figure 5.7- 4 Fracture surface of aged GB 8cm sample.....	51
Figure 5.7- 5 EDS mapping of aged as received sample	52
Figure 5.7- 6 Elemental composition of aged as received sample	53
Figure 5.7- 7 EDS mapping of aged, degreased sample	54
Figure 5.7- 8 Elemental composition of aged, degreased sample.....	55
Figure 5.7- 9 EDS mapping of aged GB2cm sample.....	56
Figure 5.7- 10 Elemental composition of aged GB2cm sample	57
Figure 5.7- 11 EDS mapping of aged GB 8cm sample.....	58
Figure 5.7- 12 Elemental composition of aged GB 8cm sample	59

List of Tables

Table 1.4- 1 Surface Pretreatments Classification	4
Table 3.1- 1 Chemical compositions of EN AW-6061 T6.....	10
Table 3.1- 2 Mechanical Properties of EN AW-6061 T6	10

Chapter:1

Introduction

1.1 Need for adhesive joining

Adhesive joining of hybrid materials is essential for light weight constructions in the aircraft and automobile industries. When compared to traditional joining procedures such as welding, brazing, and mechanical riveting, adhesive joining has various advantages. Even though mechanical riveting is the most common method for joining together aircraft assemblies, it has a drawback: compared to bonded joints, it can cause points of high stress concentration, which can result in premature failure, especially in fatigue conditions. Secondly, welding can solve many of the problems that arise when aerospace materials are joined with riveting. But some people have said that some aerospace alloys are ‘unweldable’ because such heat-treated alloys can experience solidification cracking[1-7].

Adhesively bonded joints, on the other hand, are said to be superior to mechanically fastened joints in several ways, such as having a high strength-to-weight ratio, a longer fatigue life, a simpler design, a smooth finish on the outside, and the ability to connect materials with no similarity. Aluminums adhesive bonded joints are very important in the aircraft and car industries because they have a high strength-to-weight ratio, good corrosion resistance, are easy to find, are cheap, and look good[8-11].

1.2 Surface pretreatment role in adhesive joining

Even though adhesive joining has many benefits over other traditional ways of joining, it also has some problems. In a hydrothermal environment, the mechanical performance of adhesively bonded joints gets much worse. As during the service life of adhesively bonded joints fuels used in industries, oils and some other deicing agents are used more often which may results in their fracture or damage. Experience with adhesive bonding has shown that the main point of attack in these joints is where the metal, or metal oxide, meets the polymer. Also, the rate of hydrothermal attack at the interface regions can be

sped up by service loads. Without a stable metal-polymer interface, even the best joint designs can't make sure whether the adhesive bonded joints will be durable or not[12]. The only two ways by which high joint durability can be accomplished is either by preventing corrosive substances like water from getting into the joint, like by sealing it, or by making the interface between the metal and polymer joints stronger so that water does not break them. Several studies have shown that surface pretreatments are the most important factor in how well and how long adhesively bonded joints stay together[1, 12-16]. In order to get a better bond between the substrate and the adhesive, surface pretreatments should not just be thought of as a way of cleaning the surface[12]. It is a necessary condition, but it is not enough on its own. Its functions include increasing surface energies for better wetting, changing surface chemistry to provide specific functional groups for physical or, preferably, chemical bonding, making new oxides with better resistance to water, making surface structures to increase bonding surface area, and providing features for mechanically locking polymers and making interfaces tougher[1, 8, 17].

1.3 Aluminum and its alloys

1.3.1 Aluminum

Aluminum is the third most common element in the earth's crust. Since it reacts with other elements, such as iron, oxygen, or silicon, it is often found with those things. Bauxite ore is used to get aluminum as a metal in a cost-effective way. Aluminum is popular in the aircraft industry because it is a light metal with a low density (2.7 g.cm^{-3}) and a high mechanical strength[18]. When metal meets oxygen, an oxide layer forms on its surface. This makes the metal highly resistant to corrosion. This layer is waterproof and does not let water in. In the future, it can keep the base material from oxidizing. Even though this oxide layer cannot be eaten away by acid solutions, alkaline solutions can. It can be made better through the anodizing process, which increases its thickness. Pure aluminum has a low mechanical strength, between 7 and 11 MPa, but it can be raised to around 690 MPa by heating and mixing it with other metals. But most of the alloying elements that make it stronger mechanically also make it less resistant to corrosion. So, surface treatments are needed to give the right amount of protection.

1.3.2 Aluminum alloys

As was already said, pure aluminum cannot be used to make structures because it does not have enough strength. Because of this, it is not used in industry in its pure form. Instead, it is mixed with other materials to improve performance. Silicon, magnesium, manganese, zinc, and copper are the most common[18]. The aluminum alloy studied in this thesis is EN AW-6061-T6.

1.4 Surface pretreatments

Metal substrates are subjected to a variety of surface pretreatments. On industrial surfaces that stick together, you can find lubricants, corrosion inhibitors, dust, corrosion products, salts, water that has stuck to the surface, and other contaminants. Solvent degreasing is a simple surface pretreatment that removes some of the loose surface contaminants, which can help with initial adhesion[13]. However, solvent degreasing will not be enough to make sure that adhesive-bonded joints last in harsh environments, so it can be used as a supplement to more advanced treatments.

Wet chemical pretreatments like chromic acid etching (CAE), Forest Product Laboratory (FPL), Sulfo-ferric acid (P2), phosphoric acid anodizing (PAA), and chromic acid anodizing (CAA) are used to make sure that adhesively bonded aluminum joints will stay stable over time. In these pretreatments, dangerous chemicals like strong acids or hexavalent chromium are used. These dangerous chemicals are very toxic and hard to get rid of, especially in CAE and CAA.

These wet chemical pretreatments can be replaced by physical pretreatment like Grit blasting and Physiochemical treatments like laser and plasma, they also show some promising results[17, 19-25].

The classification of common surface pretreatments is shown in Table 1.4-1 [26, 27].

Table 1.4- 1 Surface Pretreatments Classification

Physical	Physiochemical	Chemical	Electrochemical
<ul style="list-style-type: none"> • Grit blasting • Grinding 	<ul style="list-style-type: none"> • Laser • Plasma • Ion beam enhanced deposition (IBED) 	<ul style="list-style-type: none"> • Chromic acid etch (CAE) • Sulfo-ferric acid (P2) • Forest Product Laboratory (FPL) • Alkaline etch 	<ul style="list-style-type: none"> • Phosphoric acid anodizing (PAA, AC or DC) • Chromic acid anodizing (CAA) • Sulfuric acid anodizing (SAA, AC or DC) • Boric sulphuric acid anodizing (BSAA), etc.

1.4.1 Degreasing (DG)

Before doing the rest of the surface treatments, the first steps are to clean and remove grease. The main goal of degreasing is to get rid of any dirt that may have gotten on the surface of the metal while it was being moved or handled.

Solvent degreasing (DG), a simple surface pretreatment, can remove some of the loose surface contaminants and give a good initial adhesion, but it does not help with the surface modifications that are needed for adhesively bonded joints to last in harsh environments. DG should be used to supplement treatments that are more advanced[8].

1.4.2 Grit Blasting

Grit Blasting also known as Sand Blasting is a Mechanical treatment process which employs centrifugal force from a mechanical device to propel blasting media (alumina or silica grit) upon the part being blasted.

Compressed air sends small, angular, or spherical particles in the direction of a part. The type of the blast media which involves its shape, size, density, and hardness are considered very important. The pressure at which the blasting media is striking the workpiece the distance between the blaster and the workpiece, and the angle of impact plays a vital role in this process.

Hand cabinets, automated enclosures, and blast rooms are built to handle parts that come in different sizes and shapes. The containment systems are made so that the blast media and parts stay inside the enclosures and are controlled by the systems. Using gravity, the blasted material falls to a place where it can be collected and used again for blasting. This is how the enclosure systems work[28].

Grit blasting is a great way to clean and get surfaces ready. It can be used to clean rust, corrosion, and oil lubricants from the surface of metal.

1.4.3 Phosphoric acid anodizing (PAA)

A native oxide or hydroxide coating can be form on the surfaces of non-ferrous metals like aluminum, these native oxide coating provides limited protection to surface degradation.

Anodizing, which is an electrochemical process provides a thicker, durable, corrosion and wear resistant anodic oxide coating[29], [30].

In anodizing process, the components which is to be anodized is immersed in an electrolyte of suitable condition which in our case is 10wt.% of Phosphoric acid solution as we are doing Phosphoric acid anodizing PAA. After immersion in electrolyte the components are then connected to anode which is a positive electrode and the counter electrode (cathode) used can be sheet or rod of stainless steel, carbon, lead, platinum, or any other metal. This counter electrode should be inert in the anodizing electrolyte. A DC source is used to provide the required voltage.

After PAA, a new layer of anodic coating forms on the surface of the substrate. This layer makes a great base for adhesion bonding[30], [31].

1.5 Aims & objective

- To study the influence of different surface pretreatments and their parameters on the morphology and topography of the Aluminum alloy-6061.
- To study the impact of roughness and surface area on the surface adhesion and hydrothermal durability of the adhesively bonded joints.
- Fracture analysis to determine the possible adhesion mechanism.

Chapter:2

Literature Review

Researchers have used different surface pretreatments, such as mechanical methods, chemical etching, physiochemical surface treatments, and electrochemical surface treatments[31], to improve adhesive bonding properties of various aluminum alloys. A. Spaggiari A. et al. [32] and SG. Prolongo et al[33]. used mechanical treatment to change the surface morphologies of aluminum substrates. They found that making surfaces rougher makes adhesively bonded joints stronger. Researcher N. Saleema et al[34]. studied that very high adhesion strength of aluminum alloy 6061 was achieved after a very short exposure of the plasma treatment, when it was treated with atmospheric pressure helium oxygen plasma at room temperature. S. Sharifi Golru et al. [35] did some research and found that different ways of cleaning the surface of aluminum alloy 1050 improved its adhesion performance and surface hydrophilicity. Thomas S. Williams et al. [36] used helium/oxygen plasma at atmospheric pressure to treat the surface of aluminum 2024 before adhesive bonding. They found that the wettability and lap shear strengths of the joints were significantly improved.

Researchers investigated the anodization process, which is a common way to treat the surface of aluminum and produces great surface morphology and high bonding performance. Yiwei Xu et al. [37] did phosphoric acid anodization (PAA) on aluminum alloy-2060 using different parameters[38]. They found that the roughness and microstructure formed had a big effect on the bonding performance and joint durability of the pretreated alloy. L. Goglio [39] and his colleagues studied how degreasing and anodizing affect the durability of bonded joints when exposed to the environment. They found that anodized samples have the best durability because their strength stays constant over period. A. Rudawska [28] and her colleagues looked into how sandblasting affected the strength of the adhesive bonded joints between the three types of aluminum alloy sheets. The samples were blasted at three different pressures. It was found that when the same pressure was used to sandblast different types of aluminum alloys, the roughness parameters Ra and Rz were different depending on the type of alloy, and that heat

treatment made the joints in an aluminum alloy sheet twice as strong. By grit blasting mild steel and aluminum alloy with different alumina grits, A.F. Harris et al. [27] were able to learn a lot about their surface characteristics. He said that the changes in the surface's physical and chemical properties caused by the grit-blasting process had a significant contribution to the joint behavior.

Over the years, most research has been done on how to improve adhesion bonding with a single surface treatment process. However, the effects of combined treatments like anodizing and grit blasting are rarely talked about in papers about the same topic.

Comprehensive mechanistic studies on the surface characteristics and adhesion strength of bonded joints by the combined effect of surface treatment have yet to be finished or presented.

Yibo Li [40] and his colleagues looked into how the adhesion performance and surface characteristics of aluminum-lithium alloy sheets changed when the surface was treated with grit-blasting and phosphoric acid anodization (PAA) at the same time. He looked at samples that had been given different surface pretreatments and compared their wettability, how they broke, and how strong they were when pulled apart. The test results showed that the combined treatment gave good wettability and single-lap joint performance and had high surface free energy values.

Lei Dong and his colleagues also looked at how surface pretreatment on 6061 aluminum alloy sheets worked and their combined effect. He first used 400-mesh sandpaper to mechanically polish the aluminum substrate to remove the natural oxide film that formed the microgroove structure. The same substrate was then treated with phosphoric acid anodizing (PAA) process to improve the strength of the adhesive bond. The results of his experiments showed that the joint between aluminum alloy 6061 and thermoplastic adhesive can be made to fracture in a different way by using the phosphoric acid anodizing (PAA) process under the right conditions. The shear strength of the joint is also improved because the surface of the aluminum alloy has the right number of circular pits structure. Solvent degreasing is a simple surface pretreatment that removes some of the loose surface contaminants, which can help with initial adhesion. However, solvent degreasing is not enough to ensure the long-term durability of adhesively bonded joints in severe

environments, therefore surface pretreatment using solvent degreasing can be used as a supplement to more advanced treatments.

Wet chemical pretreatments like chromic acid etching (CAE), Forest Product Laboratory (FPL), Sulfo-ferric acid (P2), phosphoric acid anodizing (PAA), and chromic acid anodizing (CAA) are used to make sure that adhesively bonded aluminum joints will stay stable over time. In these pretreatments, dangerous chemicals like strong acids or hexavalent chromium are used. These dangerous chemicals are very toxic and hard to get rid of, especially in CAE and CAA. These wet chemical pretreatments that are bad for the environment are also against the law in the European Union.

Instead of using chemicals that are bad for the environment, Grit Blasting and anodizing can be used together. When First Grit Blasting is used on the surface of an aluminum alloy, the natural oxide layer on the alloy is removed by the intense collision of abrasive media, leaving a uniform layer of rough surface with dense ridges, grooves, and undercuts. Such rough spots increase the surface area of the aluminum alloy substrate. When anodizing is done on this surface, it forms porous and cellular nano structures. This makes the bonding area bigger because the treated surface has structures on both the micro and nano scales. This also increases the shear strength. Yibo Li et al. [40] said that after anodizing porous structures are formed, but what actually happens is that cellular nanostructures also form, which increases the bonding area.

Chapter:3

Experimental Procedure

3.1 Materials

Aluminum alloy EN AW-6061-T6 was used as a substrate material and all the studies were performed on this alloy. The chemical composition of the alloy is given in Table 3.1-1 and Table 3.1-2 shows its mechanical properties. Polyamide or Nylon 6 (PA6) was used as a thermoplastic hot melt adhesive which was supplied by mf folien GmbH.

Table 3.1- 1 Chemical compositions of EN AW-6061 T6

Element	Si	Fe	Cu	Mn	Mg	Ti	Cr	Zn	Others	Al
wt %	0.56- 0.70	0.30 (max)	0.18- 0.32	0.10 (max)	0.84- 1.02	0.02 (max)	0.10- 0.20	0.02 (max)	<0.15 %	Remainder

Table 3.1- 2 Mechanical Properties of EN AW-6061 T6

Tensile Strength (MPa)	Yield Strength (MPa)	%Elongation (GL- 50mm)	Hardness (HV)
300-314	270-280	12-13	106-110

3.1.1. Dimensions of Specimen

The material purchased was in the form of sheets having dimension (500 × 300 × 1.5 mm³) as shown in Figure 3.1-1.



Figure 3.1- 1 EN AW-6061 T6 Sheet

The dimension for each aluminum specimen which we needed for the surface pretreatment were ($72.5 \times 10.0 \times 1.5 \text{ mm}^3$). Therefore, the aluminum sheets were cut into required dimensions by CNC Laser cutting machine present in Robot Maker lab EME college NUST. Figure 3.1-2 shows the aluminum sheet during laser cutting and aluminum strips after laser cutting are presented in Figure 3.1-3.



Figure 3.1- 2 Laser Cutting of EN AW-6061 T6 Sheet



Figure 3.1- 3 EN AW-6061-T6 Sheet after Laser cutting

3.2. Surface pretreatment

3.2.1. Degreasing

For degreasing, the sample were placed in a beaker containing high purity acetone. The beaker was then placed in ultrasonic bath for 10 minutes in 2 cycles, each time using a fresh acetone solvent. To remove any type of residues, present at the specimen surface, the samples were dipped in fresh acetone after the second cycle. Before adhesive bonding the samples were air dried. Note that the samples labeled as received (AR) did not get any type of surface pretreatment even degreasing.

3.2.2. Grit Blasting

Grit blasting was carried out using a mixture of alumina and sand as grit with mesh size 40 μ m. All the samples were blasted at a constant pressure of 5 bar for 10 sec. The grit was blasted at an angle of 90° to the surface of the sample. The distance between the sample and the grit exit nozzle was either 2cm or 8cm and accordingly samples were designated as GB2 or GB8. The blasted samples were then cleaned in ultrasonic bath containing high purity acetone for 2 cycles each of 10 minutes so that any slack grit particles may be

removed from the grit blasted surface. And before using the samples for adhesive bonding they were air dried [41].

3.2.3. Phosphoric acid anodizing (PAA)

The standard Phosphoric acid anodizing (PAA) surface pretreatment was performed according to another study [42] and the procedure is shown in the form of flow chart in Figure 3.2-1. After degreasing and alkaline etching, the samples were cleaned with deionized (DI) water and dried before anodizing.

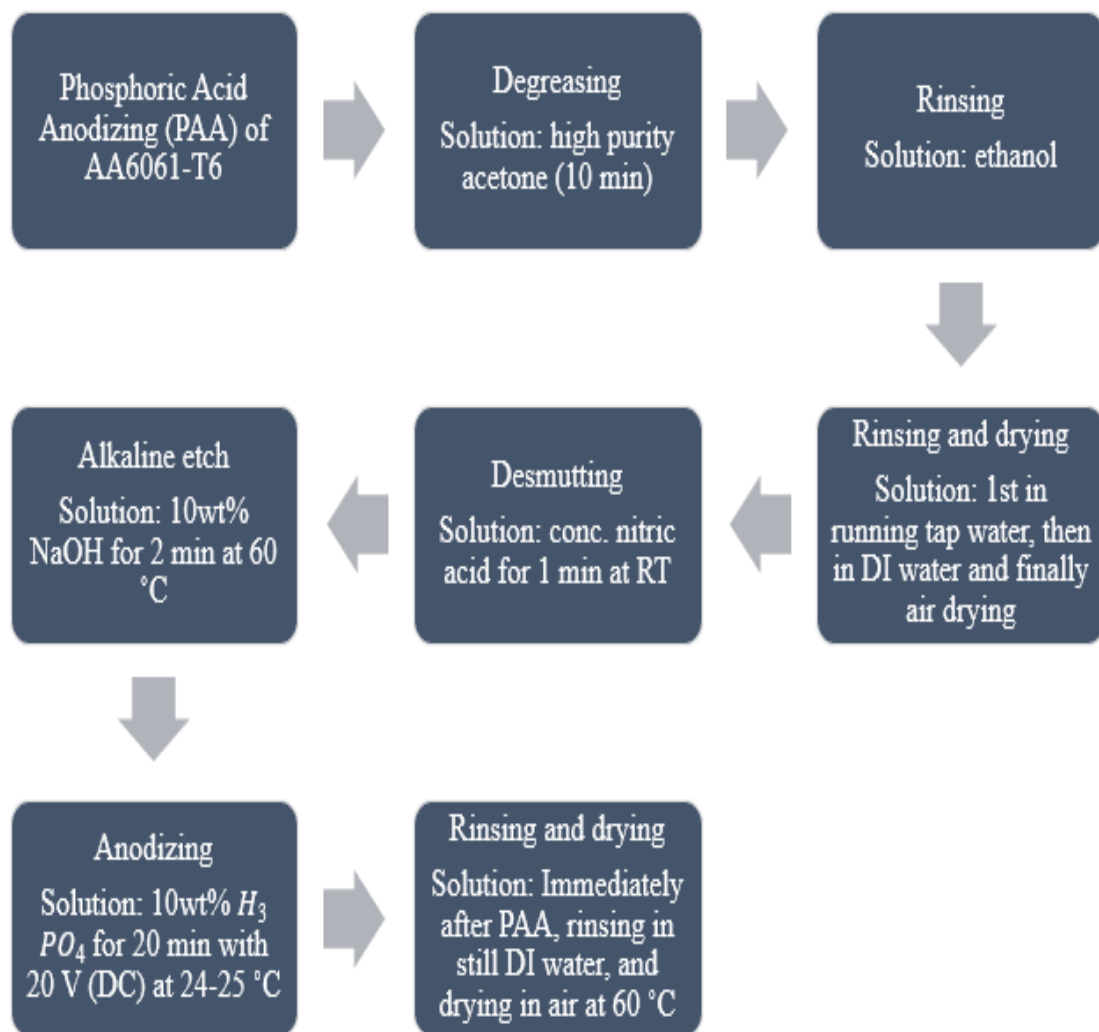


Figure 3.2- 1 Standard PAA pretreatment flow chart

The phosphoric acid anodizing (PAA) was performed in an electrochemical cell using 10wt% H₃PO₄ was used as an electrolyte. The cathode was a plate of stainless steel (SS)

and the aluminum strips were connected with the positive terminal of the DC source as anode [42]. A setup was developed, as shown in Figure 3.2-2, to hold the samples and the SS plate. The voltage was raised to 20 V at a rate of 1 V/30 s and held there for 20 minutes. The samples were rinsed in deionized water after the anodizing was complete. Before using the samples for adhesive bonding, they were dried in an oven at 60 °C for 15 minutes.

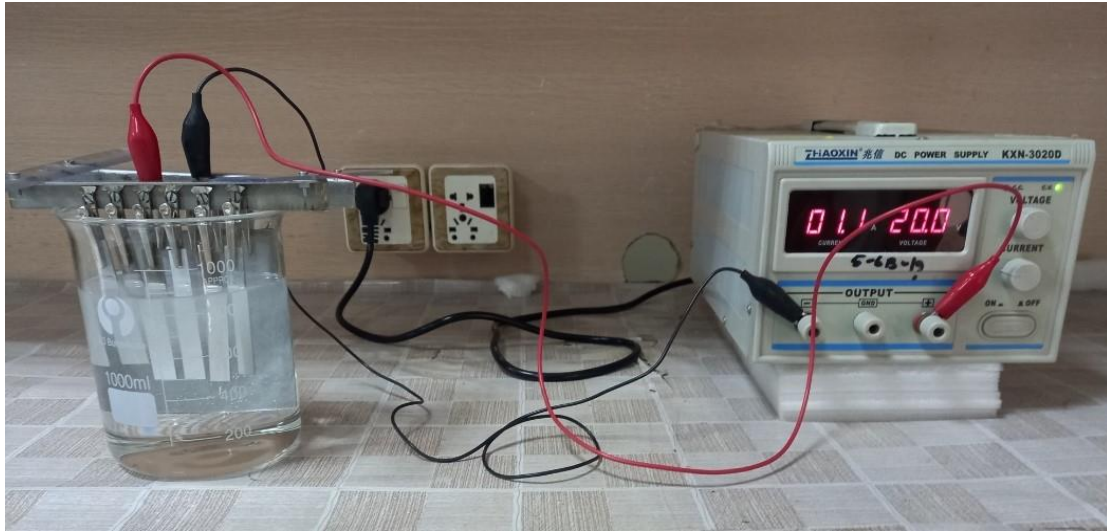


Figure 3.2- 2 Phosphoric acid anodizing Setup

3.3. Adhesive Bonding process

For adhesive bonding process a tool was designed and manufactured from a brass plate. The tool was manufactured as per the dimensions of the joints so that it can hold the bonding assemblies, shown in Figure 3.3-1.

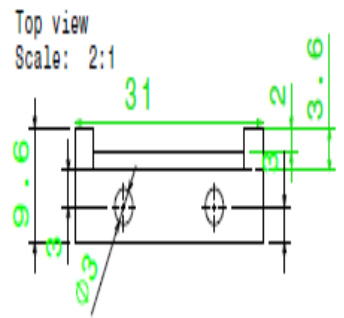
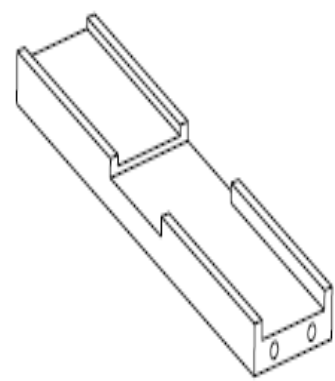
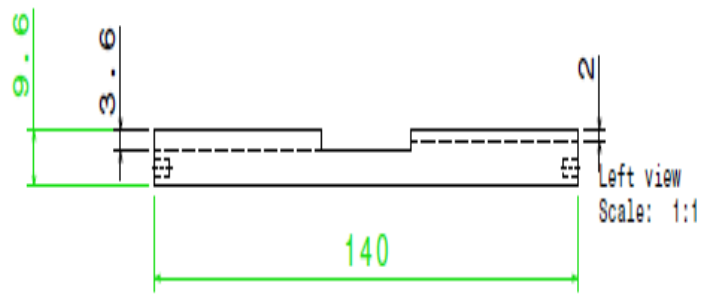
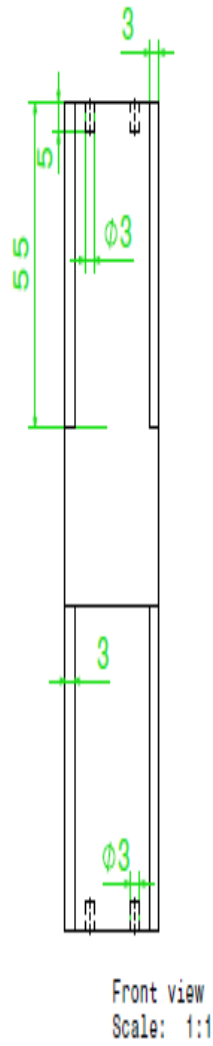


Figure 3.3- 1 Bonding tool for Adhesive Joints

3.3.1. Design and Fabrication of bonding tool

Before manufacturing the bonding tool, the design was made in CATIA which is a CAD design 3D software used in a variety of industries, including aerospace and automotive, to design, simulate, analyze, and manufacture products.

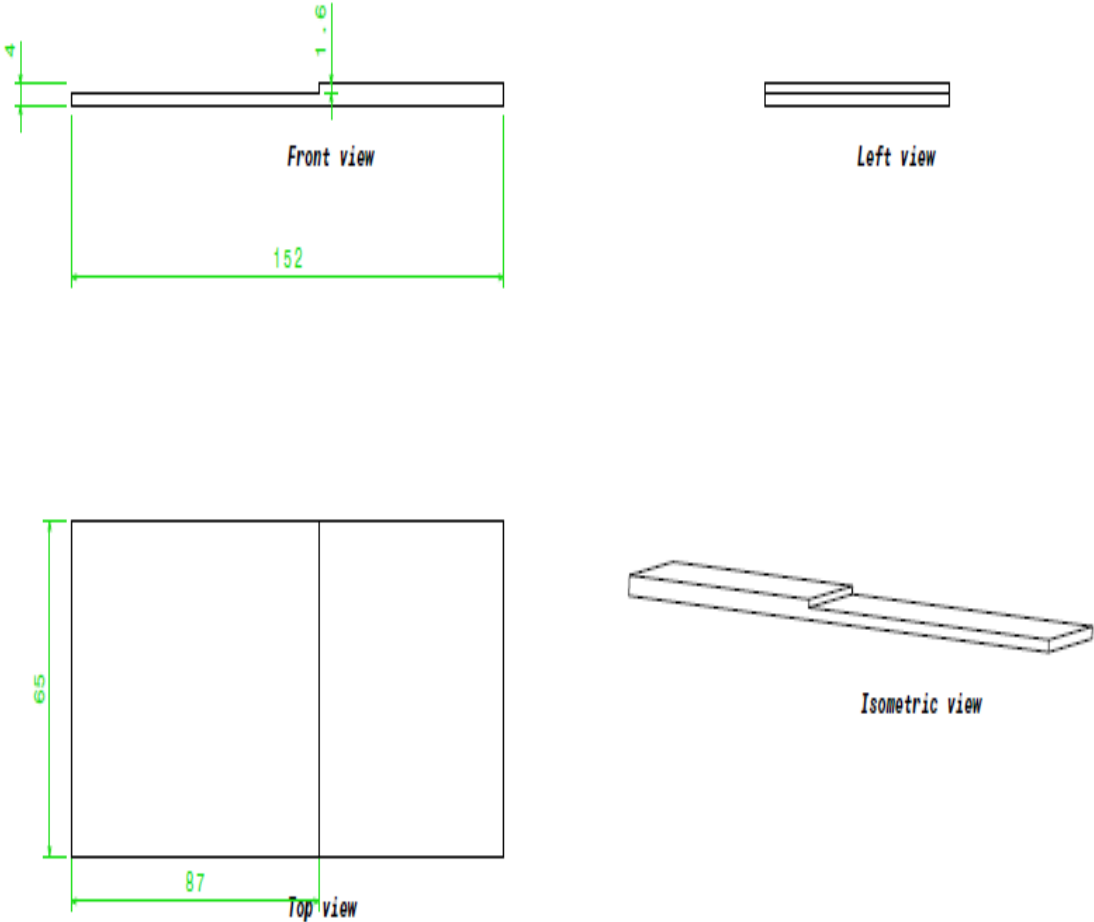
The first design of the bonding tool which is shown in Figure 2.3-2 was perfect to hold the bonding assemblies, but unfortunately, we could not manufacture that design because the brass sheet of the required thickness of 9.6mm was very expensive.



DESIGNED BY: Usama Naeen			
DATE: 11/8/2021			
CHECKED BY: Dr. M Irfan			
DATE: 11/8/2021			
FILE: A3		DASSAULT SYSTEMES	
SCALE: 1:1	WEIGHT (kg): 0.266	ISSUING NUMBER: lower part mold	SHEET: 1/1

Figure 3.3- 2 First design of Bonding tool

Therefore, a new design of bonding tool, see 2D drawings in Figure 3.3-3, was made from a relatively thin brass plate. The 3-D drawing of bonding tool is shown in Figure 3.3-4.



DESIGNED BY: Usana Naeem		I	-
DATE: 11/14/2021		H	-
CHECKED BY: Dr. M Irfan		G	-
DATE: 11/14/2021		F	-
		E	-
SIZE: A3		D	-
		C	-
SCALE: 1:1	WEIGHT (KG): 0.03	WORKING NUMBER: Part1	SHEET: 1/1
		B	-

Figure 3.3- 3 New design of Bonding tool

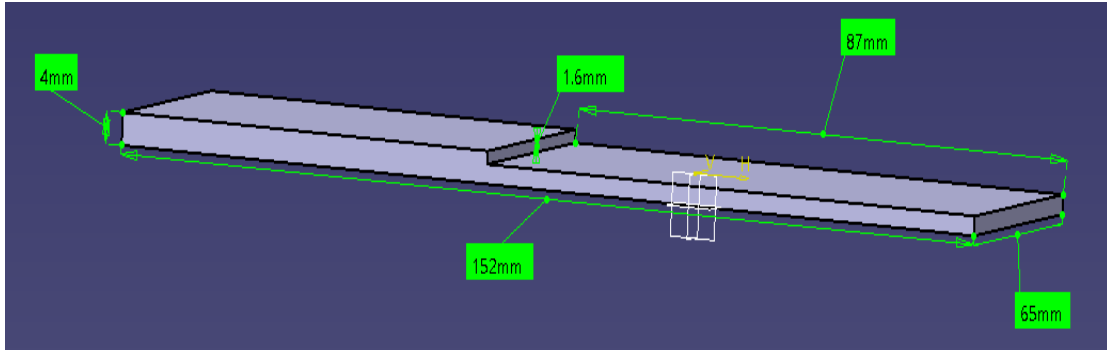


Figure 3.3- 4 3D Image of Bonding tool

A 4mm brass sheet was purchased from the local vendor and the bonding tool was manufactured by CNC Milling machine (MV-1060) present at Design and Manufacturing Engineering Department, School of mechanical and manufacturing engineering (SMME) NUST. Figure 3.3-5 shows the manufacturing of bonding tool along with the machined bonding job.



Figure 3.3- 5 Manufacturing of Bonding tool by CNC milling machine

After the bonding tool was initially manufactured then holes for M3 screws were drilled as per the dimensions of the joints so that it can hold the bonding assemblies. Figure 3.3-6 shows the drawing for the dimension at which holes for M3 screw were made.

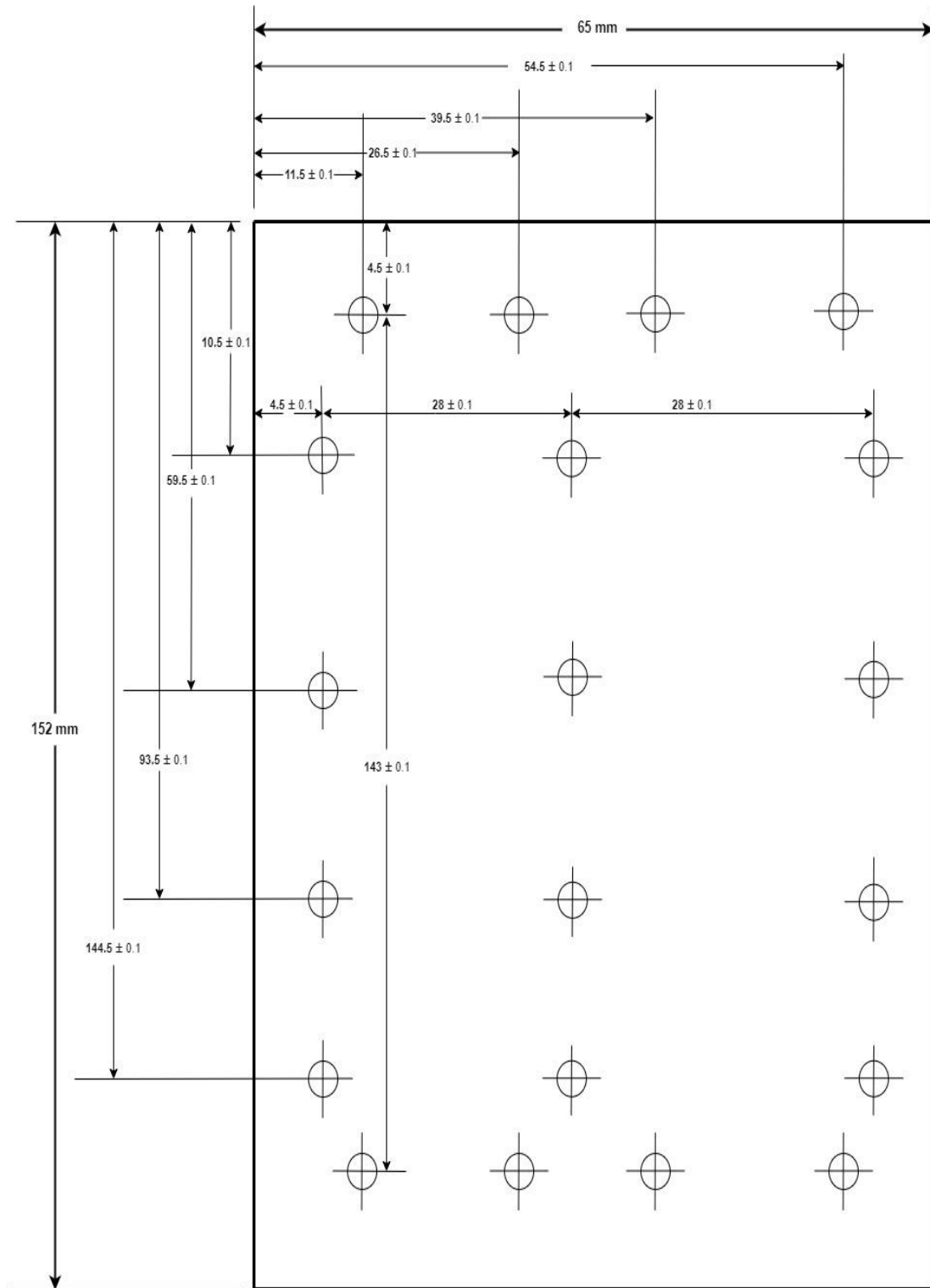


Figure 3.3- 6 Holes dimensions for m3 screw

The holes were made by milling machine available at manufacturing resource center (MRC) SMME NUST. A drill bit of 2.4 mm was used to create holes and tapping of 0.6mm was done to cut internal threads in holes so that a cap screw of size M3 can be threaded into the hole. Figure 3.3-7 shows the process of holes creation by milling machine and tapping for internal threading.



Figure 3.3- 7 M3 screw holes drilling and tapping

3.4. Thermal joining process

A convection oven (model UN30 manufactured by Memmert) was utilized to perform adhesive bonding. Before bonding PA6 adhesive was cleaned in ultrasonic bath for two cycles, each 10 min, in a solution containing 50% DI water and 50% Ethanol. After cleaning, PA6 adhesive was dried overnight in an oven at 65°C and then used for bonding aluminum substrates[8, 17].

The PA6 joints were consolidated at 225°C for 15 minutes, as per the recommendation of the manufacturer. The oven took approximately 30 - 40 min to reach 225 °C. The temperature was hold for 15 min at 225°C and after 15 min the oven door was slightly opened for 25 minutes and then left fully opened for 20 minutes to allow the joining assemblies to cool to room temperature.

For each type surface pretreatment, a set of six samples were prepared. Three samples were tested under unaged conditions and the other three samples were subjected to hydrothermal aging before testing.

Chapter:4

Characterization Techniques

4.1. Mechanical Testing

4.1.1. Single Lap Shear Joint Test

For mechanical testing a pair of aluminum substrates was adhesively bonded, the dimensions of the aluminum substrates were $72.5 \times 10.0 \times 1.5 \text{ mm}^3$, and the overlap area was $10 \times 5 \text{ mm}^2$, Figure 4.1-1. European Standard DIN EN 1465 was used to determine these dimensions and these dimensions were reduced to prevent excessive substrate deformation, which could negate the pretreatment's results.

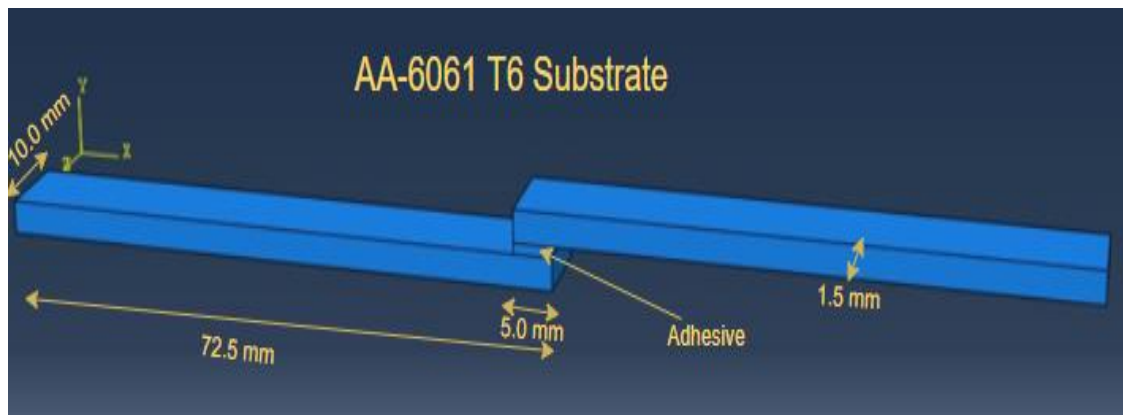


Figure 4.1- 1 Schematic of substrate for single lap joint shear test

One set of three samples was prepared for each surface pretreatment and each set was then tested under unaged condition with strain rate of 1mm/min. in Universal testing machine of (model SHIMAD2U 20KN). A load cell of 5kN was used (Figure 4.1-2).



Figure 4.1- 2 Single lap joint shear test setup

4.1.2. Hydrothermal Aging

Similarly for joint durability studies the other set was subjected to hydrothermal aging before mechanical testing. Aging of samples was done at 80 °C for 7 days. The samples were stacked in a beaker of 1000 ml containing deionized water, the beaker was then placed over a hot plate and temperature was adjusted such that the thermometer placed inside the beaker showed 80 °C. A special setup shown in Figure 4.1-3 was developed to refill the beaker when the DI water level starts to drop due to evaporation. The samples were removed from the beaker after 7 days and were tested immediately[43].



Figure 4.1- 3 Hydrothermal Aging setup

For calculating lap shear strength geometrical bonding area was used, the following relation used to calculate lap shear strength:

$$\tau_{max.} = \frac{F_{max.}}{\text{overlap length} * \text{width}}$$

4.2. Scanning electron microscopy (SEM)

The surface morphologies were studied using SEM. The pretreated samples were investigated using SEM manufactured by JEOL model (JSM6490A). Before scanning a thin layer of gold was sputtered to all the pretreated samples using a gold sputter coater to make them more conductive to facilitate the analysis. Under high vacuum, an electron beam with an acceleration voltage of 20 kV was used to scan all the samples. Secondary

electron detector was used, and images were taken at different magnification and were then investigated.

4.3. Energy dispersive x-ray spectroscopy (EDS or EDX)

Energy Dispersive X-Ray Spectroscopy is an analytical technique used in conjunction with scanning electron microscopy (SEM). EDS was used for the identification of elemental composition of individual points as well as the mapping of lateral distribution of the elements from imaged area. EDS analysis of all the pretreated samples, aged as well as unaged was done.

4.4. Optical Profilometry

An optical profilometer is an instrument for measuring the profile of a surface to determine its roughness. All the pretreated samples were scanned under optical profilometer, the result shows values for different roughness parameters. To study roughness profile, the average of the following roughness parameters was taken and plotted; R_a (arithmetic mean height), R_q (root mean square height) and R_z (Avg. Max. Height of the Profile).

4.5. Optical Microscopy

Optical microscope was used to measure the thickness of adhesive after bonding. Emery paper of different grades (P240 and P800) was first used to get smooth and shiny finished surface so that the adhesive can be easily viewed under optical microscope. Figure 4.5-1 shows the sample prepared for optical microscope by using emery paper.



Figure 4.5- 1 Sample preparation for Optical Microscope

After finishing the surface of the sample, the thickness of the adhesive was viewed under optical microscope manufactured by Optika Italy model IM-3 MET. The images were taken at a low magnification of 5X.

Chapter:5

Results and Discussion

5.1. Morphological study of un bonded pretreated surfaces: Unaged

5.1.1. As Received

SEM image of as received sample at 1000X showed sheet rolling lines at low magnification (arrows in Figure 5.1-1) and contaminants and some loose products of oxides/hydroxides on the surface of the alloy as indicated by arrows at higher magnification of 10,000X (Figure 5.1-1).

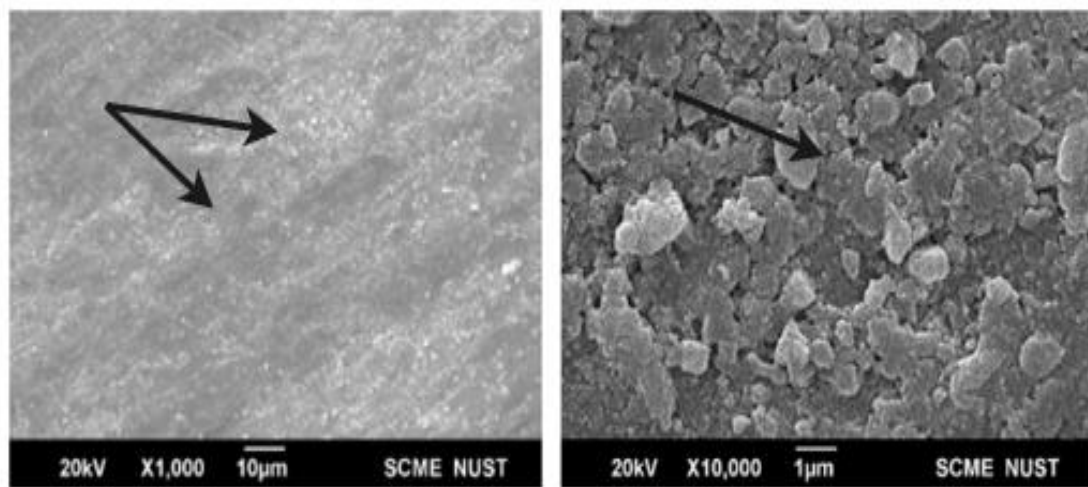


Figure 5.1- 1 SEM image of as received sample

5.1.2. Degreased

The SEM image of degreased sample at 1000X also revealed the original rolling lines of the sheet and some loose products of oxides/hydroxides on the surface of the alloy as indicated by arrows in Figure 5.1-2. At higher magnification of 5000X some cracks were also visible (as indicated by arrow in Figure 5.1-2) along with loose products.

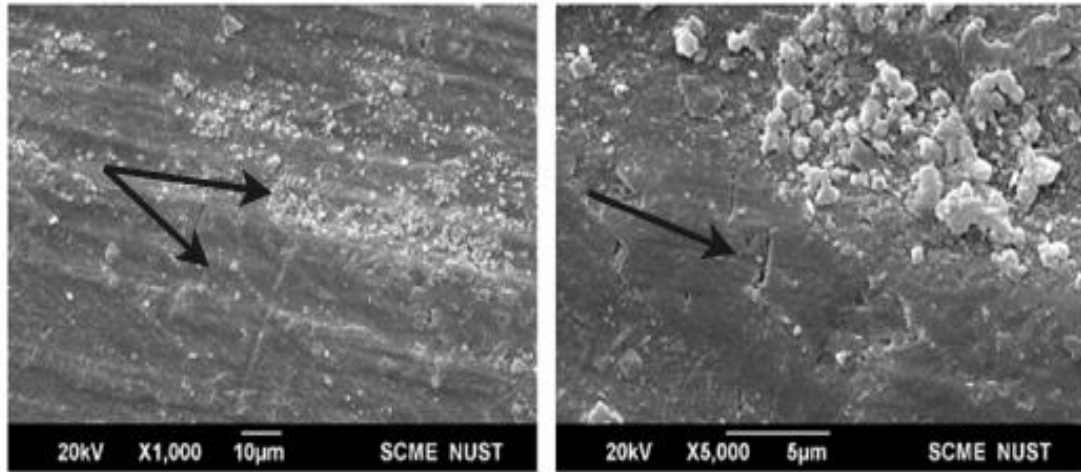


Figure 5.1- 2 SEM image of degreased sample

5.1.3. Grit Blast at 2cm Distance (GB2)

The SEM image of the grit blasted sample with sample to nozzle distance of 2cm (GB2) demonstrated a large number of undercuts and re-entrant geometries, Figure 5.1-3. The image at 5000X further revealed the under cuts and re-entrants features that may provide the sites for mechanical interlocking of adhesive at the substrate and an increase in real surface area for the physicochemical interactions between alloy substrate and adhesive, Figure 5.1-3.

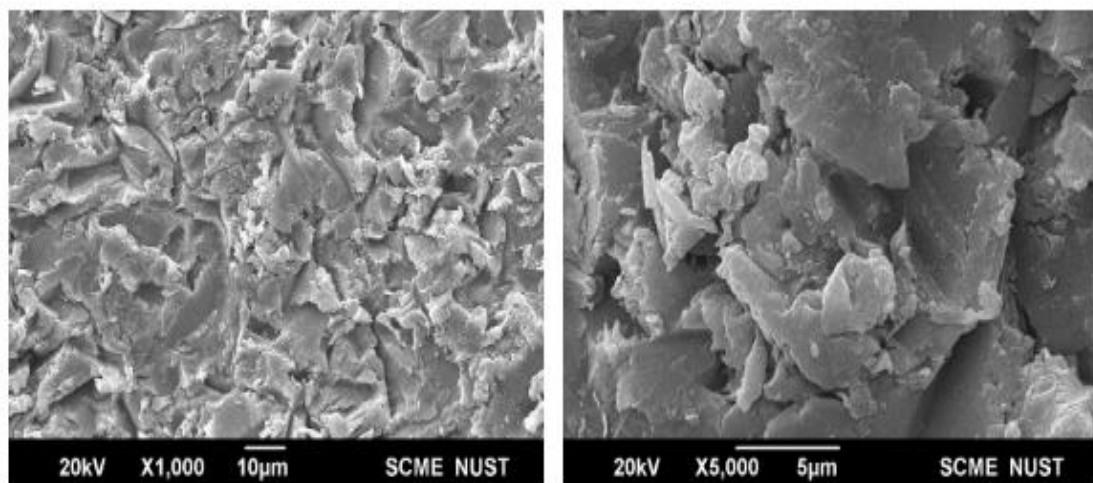


Figure 5.1- 3 SEM image of GB2 sample

5.1.4. Grit Blast at 8cm Distance (GB8)

The SEM image of the grit blasted sample, GB8, also showed the undercuts and re-entrant geometries at the surface, Figure 5.1-4.

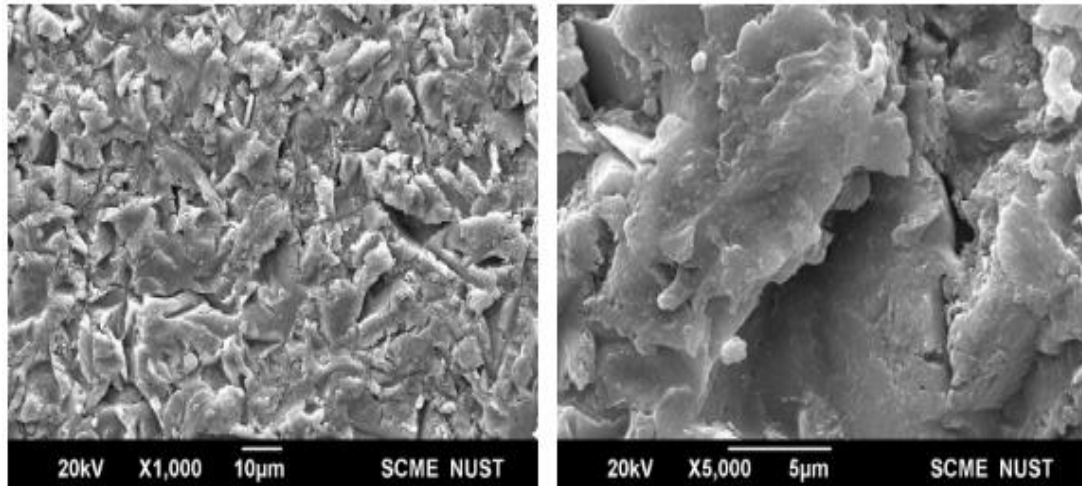


Figure 5.1- 4 SEM image of GB8 sample

5.1.5. Phosphoric acid Anodizing (PAA)

The SEM image of PAA pretreated samples taken at 1000X demonstrated dimple like micro-structures (Figure 5.1-5) which were due to chemical treatment performed before anodizing process. At higher magnification of 60,000X, cellular nanostructures were evident, Figure 5.1-5.

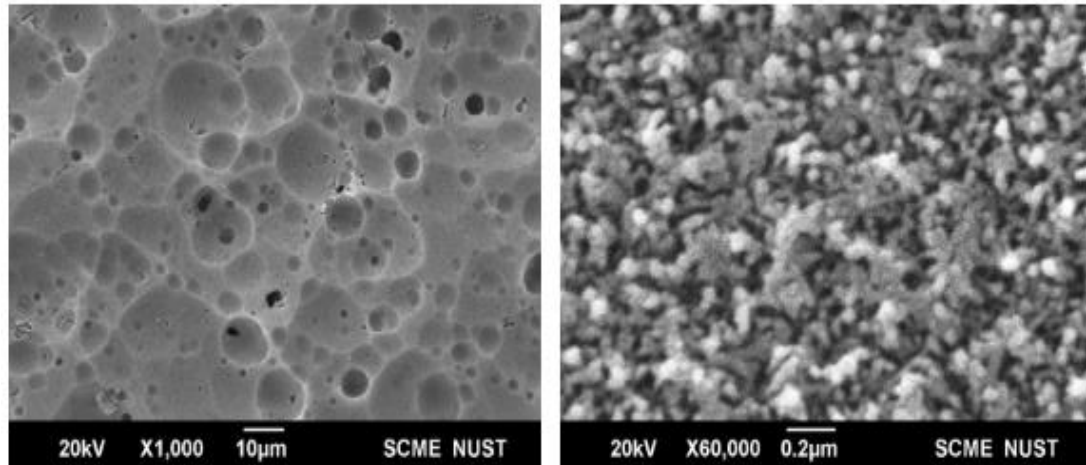


Figure 5.1- 5 SEM image of (PAA) sample

5.2. Morphological study of unbonded pretreated surfaces: Aged

5.2.1. As Received

SEM image of as received sample after hydrothermal aging showed that due to hydration various oxides/hydro oxides were formed on the aged surfaces, Figure 5.2-1.

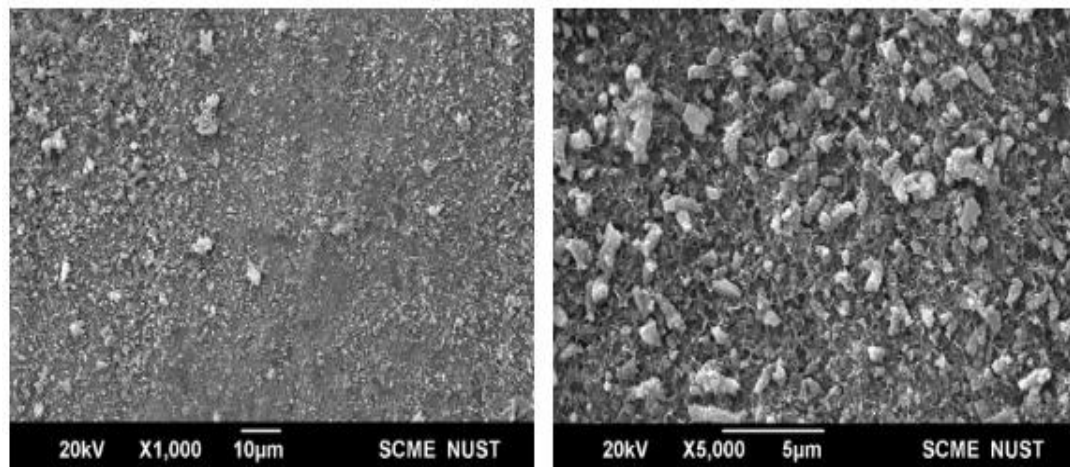


Figure 5.2- 1 SEM image of as received sample

5.2.2. Degreased

The SEM image of degreased sample also confirmed that the structure was changed some home due to hydration and some crystals of early stages of hydration were formed. (Figure 5.2-2).

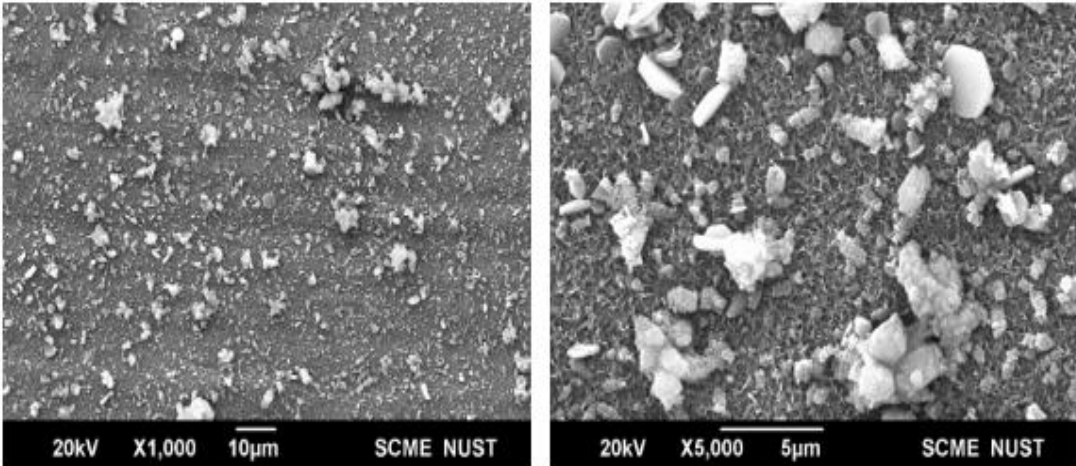


Figure 5.2- 2 SEM image of degreased sample

5.2.3. Grit Blast at 2cm Distance (GB2)

The SEM image of the grit blasted sample at 2cm distance (GB2) after aging shows that the grit blasted features were visible even after hydration, Figure 5.2-3).

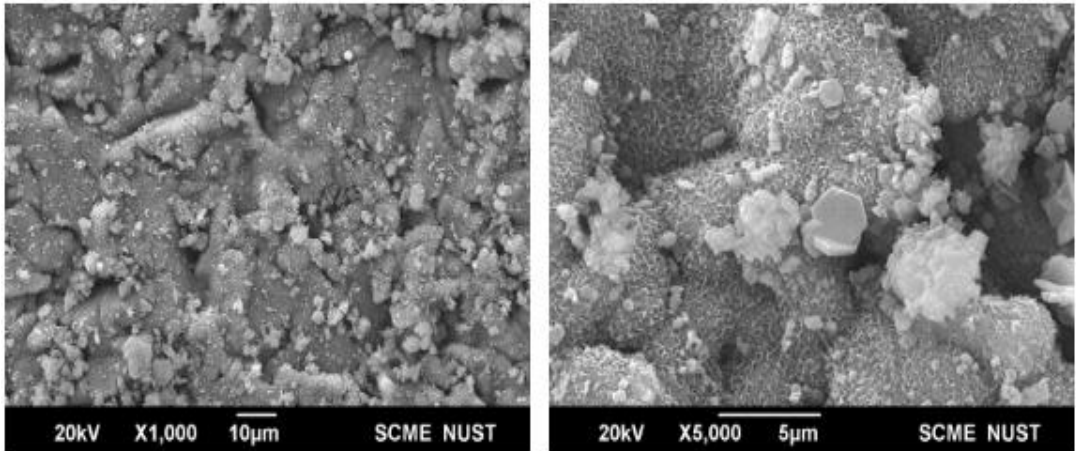


Figure 5.2- 3 SEM image of GB2 sample

5.2.4. Grit Blast at 8cm Distance (GB8)

The SEM image of the grit blasted sample at 8cm distance (GB8) also showed similar behavior like demonstrated by the samples with blasting distance of 2cm, GB2, Figure 5.2-4.

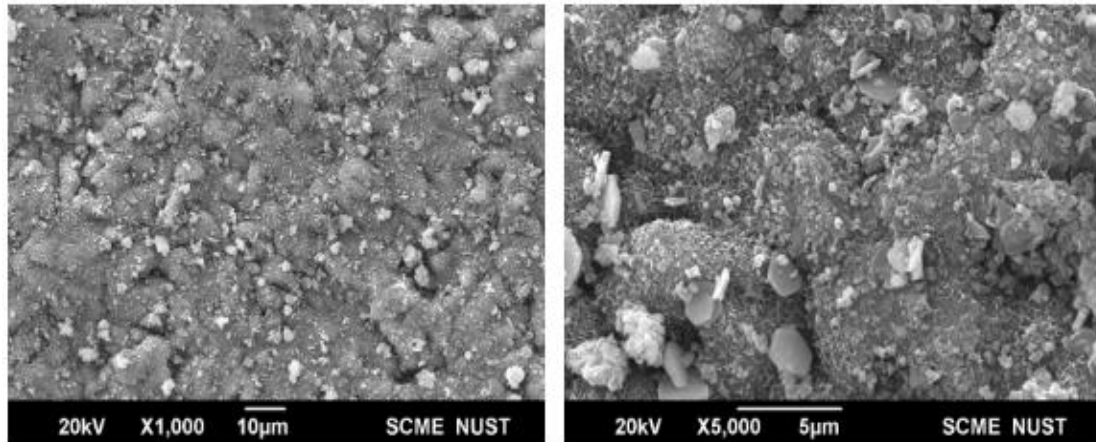


Figure 5.2- 4 SEM image of GB8 sample

5.3. Topographical Analysis

For topographical analysis surface roughness parameters Ra, Rq, and Rz of different surface pretreatments were obtained through optical profilometry technique and are shown in figure 5.3-1. As Received and degreased samples exhibited a very small surface roughness with Ra value of 0.3 µm and 0.5 µm, respectively. After treating the samples with anodization process, the Ra value increased to 1.7 µm. When the samples are subjected to grit blasting by keeping pressure constant at 5 bar and varying the distance between the sample surface and the grit exit nozzle, the surface exhibits a high roughness Ra value of 14.0 µm and 15.1 µm when the distance was maintained at 2 cm and 4 cm, respectively. When the distance was further increased to 6cm and 8 cm the Ra value again decreased to 2.2 µm and 2.0 µm, respectively. Approximately Similar trend was observed for surface roughness parameter, Rq and Rz.

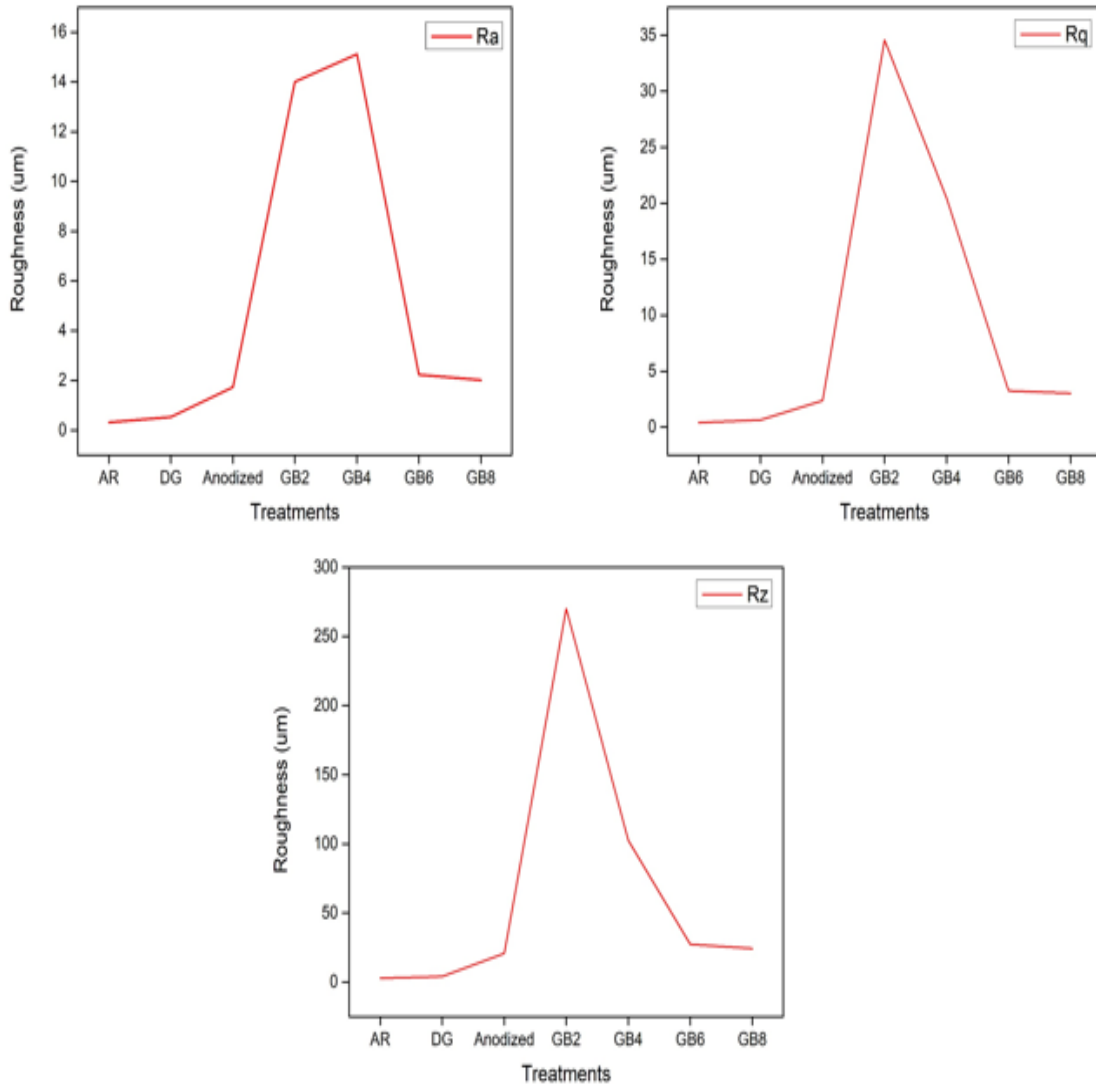


Figure 5.3- 1 Surface roughness values Ra, Rq and Rz of diff. surface treatments

5.4. Bondline Thickness of adhesively bonded joints

The bondline thickness of adhesively bonded joints of two different samples was measured using optical microscope. The figure 5.4-1 and 5.4-2 shows the image of result obtained via optical microscope. The bondline thickness was around 187 μm, 161 μm, and 142 μm for sample 1 measured at three different points, figure 5.4-1, after thermal consolidation. Similar observations were made for sample 2, figure 5.4-2 figure 5.4-2. For adhesive bonding, 2 strips of PA6 polymer adhesive having thickness 100 μm each were used, so the total thickness before the consolidation was 200 μm. But during consolidation

as the temperature was increased the polymer melted and some polymer flowed out of the bonded area and therefore the bondline thickness was lower than 200 μm after consolidation as evident from figure 5.4-1 and figure 5.4-2.

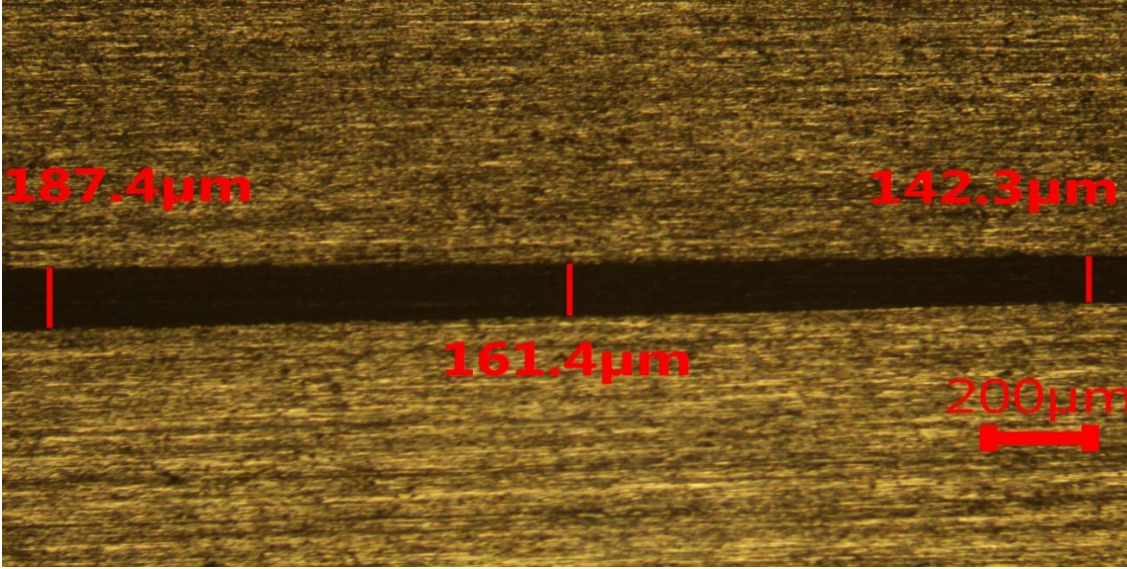


Figure 5.4- 1 Bond line of Sample 1

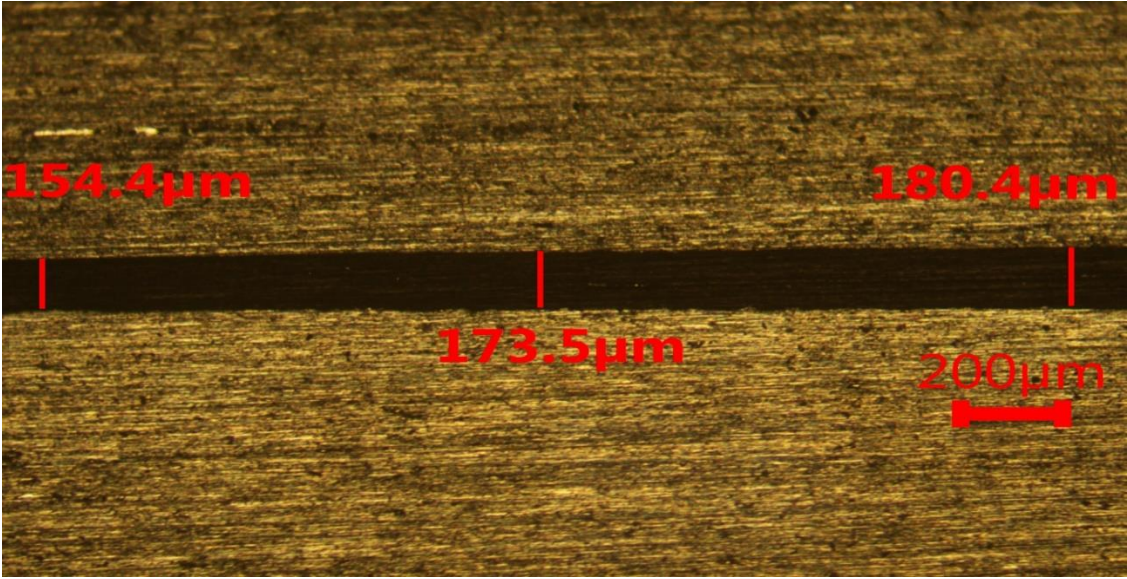


Figure 5.4- 2 Bond line thickness of sample 2

5.5. Single lap joint shear strengths

The mechanical test of adhesively bonded joints revealed that the single lap shear strength of the grit blasted samples was enhanced as compared to as received and decreased, figure

5.5-1. The AR and degreased samples showed single lap shear strength of 9.0 MPa and 13.0 MPa, respectively. The grit blasted samples demonstrated the lap shear strengths of 19.2 MPa and 12.3 MPa for GB2 and GB8 samples, respectively. The anodized sample showed lap shear strength of 15.7 MPa. The enhanced strength of grit blasted, and anodized surfaces was due to increased roughness values, see figure 5.3-1. This increased surface roughness increased the surface area and hence the adhesion strengths were enhanced.

The as received and degreased samples after hydrothermal aging showed zero strength while grit blasted samples demonstrated comparatively good strengths after the aging, figure 5.5-1. Here, the aging resistance of GB 2 samples was higher compared to the GB8, and this can be attributed to the higher surface roughness of these samples. The lower aging resistance of the anodized samples needed further investigation.

To explain the variations in adhesion strengths and aging resistance of various surfaces and to see whether the change in strength and the failure was due to chemical bonding or mechanical interlocking, the fracture surfaces were analyzed using SEM and EDX studies.

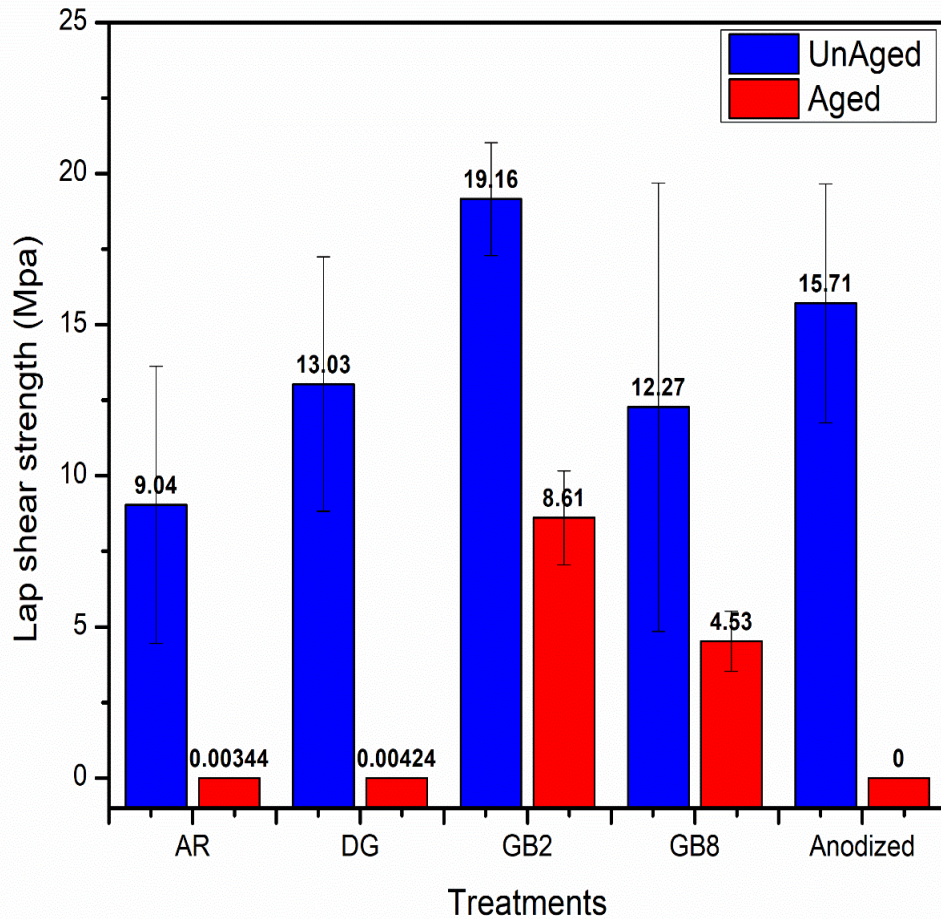


Figure 5.5- 1 Lap shear strength of Pretreated samples

5.6. Fracture Analysis: unaged samples

5.6.1. Morphological study

5.6.1.1. As Received

In Figure 5.6-1 rolling lines were evident seen on the fracture surfaces of the as received samples. These rolling lines indicated almost complete adhesive failure of the joints and hence very weak bonding between the polymer and the as received sample surfaces.

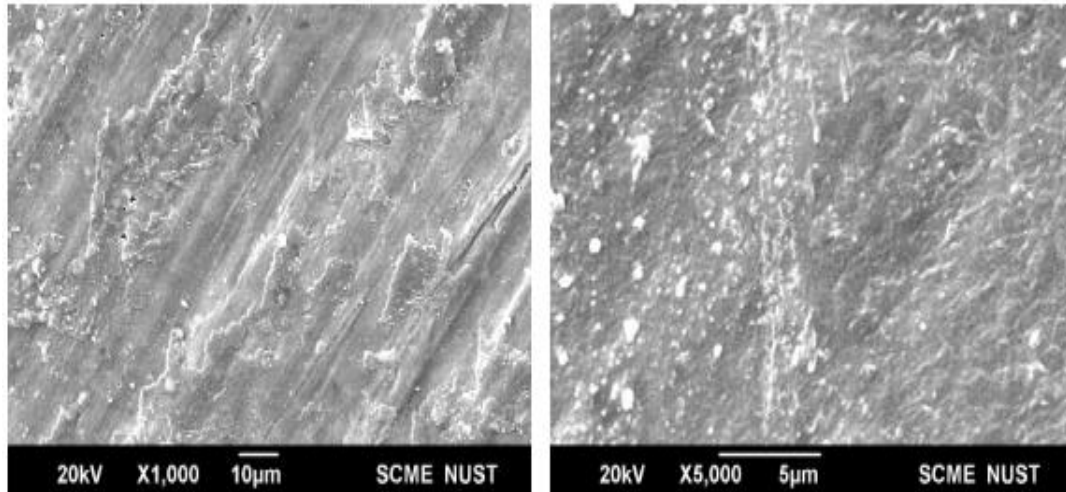


Figure 5.6- 1 Fracture surface of unaged As Received sample

5.6.1.2. Degreased

The fracture surface of unaged degreased sample also showed the original rolling lines of the sheets, Figure 5.6-2. The rolling again indicated the very weak bonding of the polymer to the degreased only surfaces. However, some polymer residues were evident at the fracture surfaces showing relatively better adhesion of polymer at these surfaces compared to the as received ones.

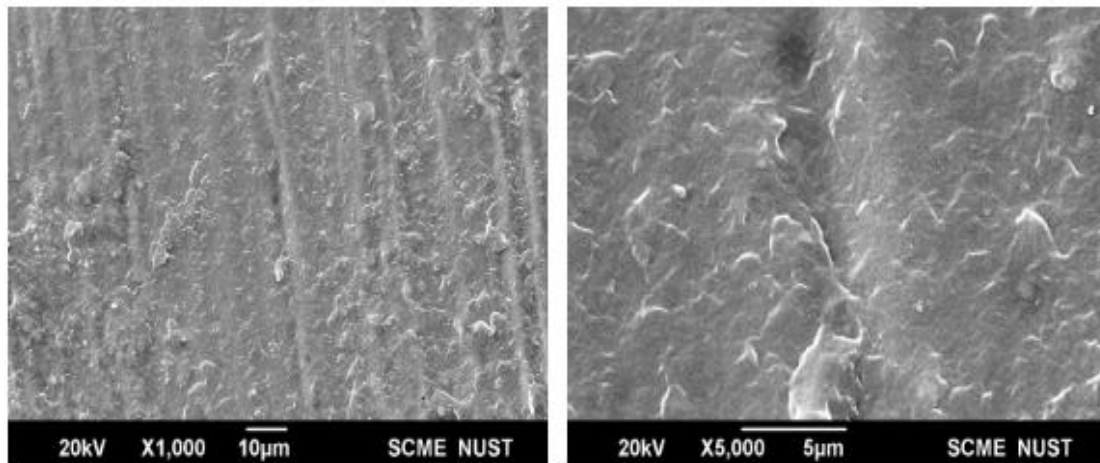


Figure 5.6- 2 Fracture surface of unaged Degreased sample

5.6.1.3. Grit Blast at 2cm Distance (GB2)

The fracture surface of unaged GB2 sample (Figure 5.6-3) revealed large polymer residues at these surfaces. Most of the polymer was locked at the undercuts generated by grit particles. This observation shows higher adhesion at these surfaces leading to cohesive failure of the joints and hence explained the higher single lap shear strengths of these joints. Therefore, the undercuts were the suitable sites available at the surface for the polymer interlocking and increased surface area resulted in large number of sites for chemical.

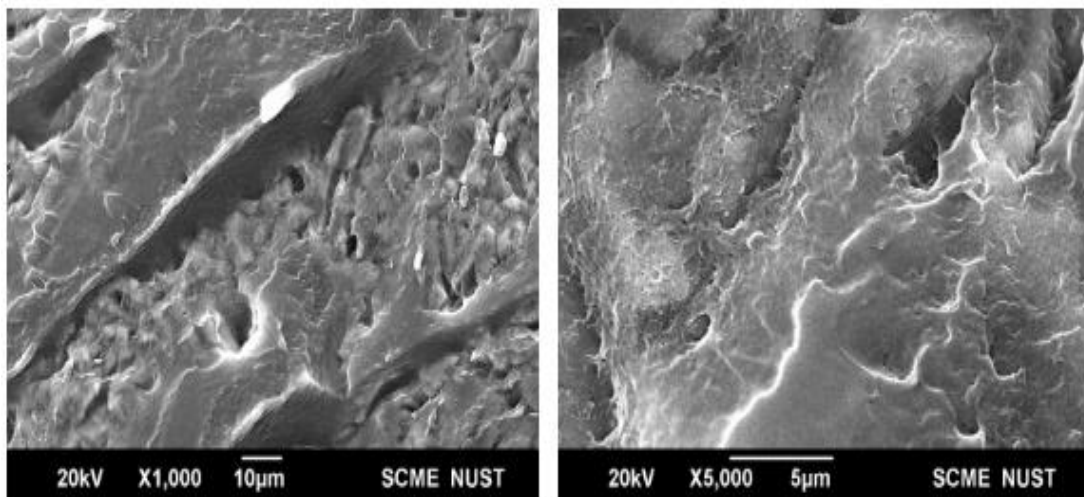


Figure 5.6- 3 Fracture surface of unaged GB2cm sample

5.6.1.4. Grit Blast at 8cm Distance (GB8)

GB8 fracture surfaces demonstrated similar behavior compared to the GB2 ones, figure 5.6-4. The difference in adhesion strengths of GB8 and GB2 can therefore be only explained by the difference in surface roughness and hence surface area of these surfaces.

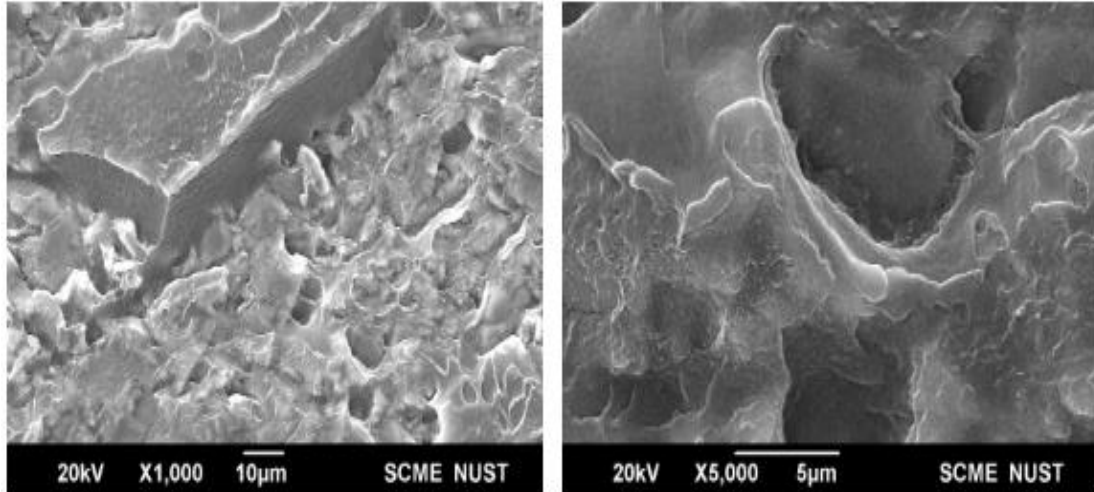
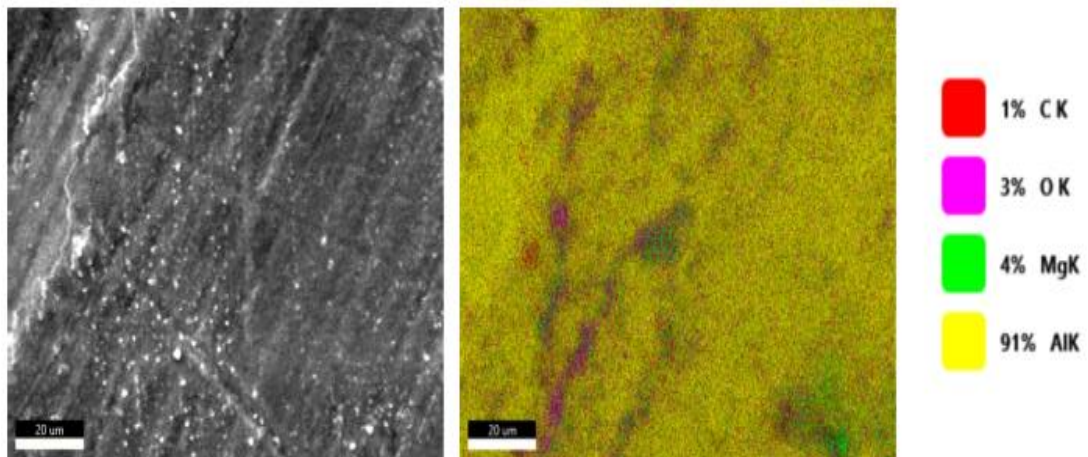


Figure 5.6- 4 Fracture surface of unaged GB8cm sample

5.6.2. Compositional study

5.6.2.1. As Received

The EDS mapping of AR samples showed the signal mostly of aluminum with very less signal from the carbon, figure 5.6-5 & figure 5.6-6. Also, it was confirmed through SEM image that the AR features, i.e., rolling lines etc. were still visible and so the failure was between metal and polymer and there was no polymer infiltration to substrate. Since all the polymer was debonded from the metal surface, therefore the failure was adhesive one.



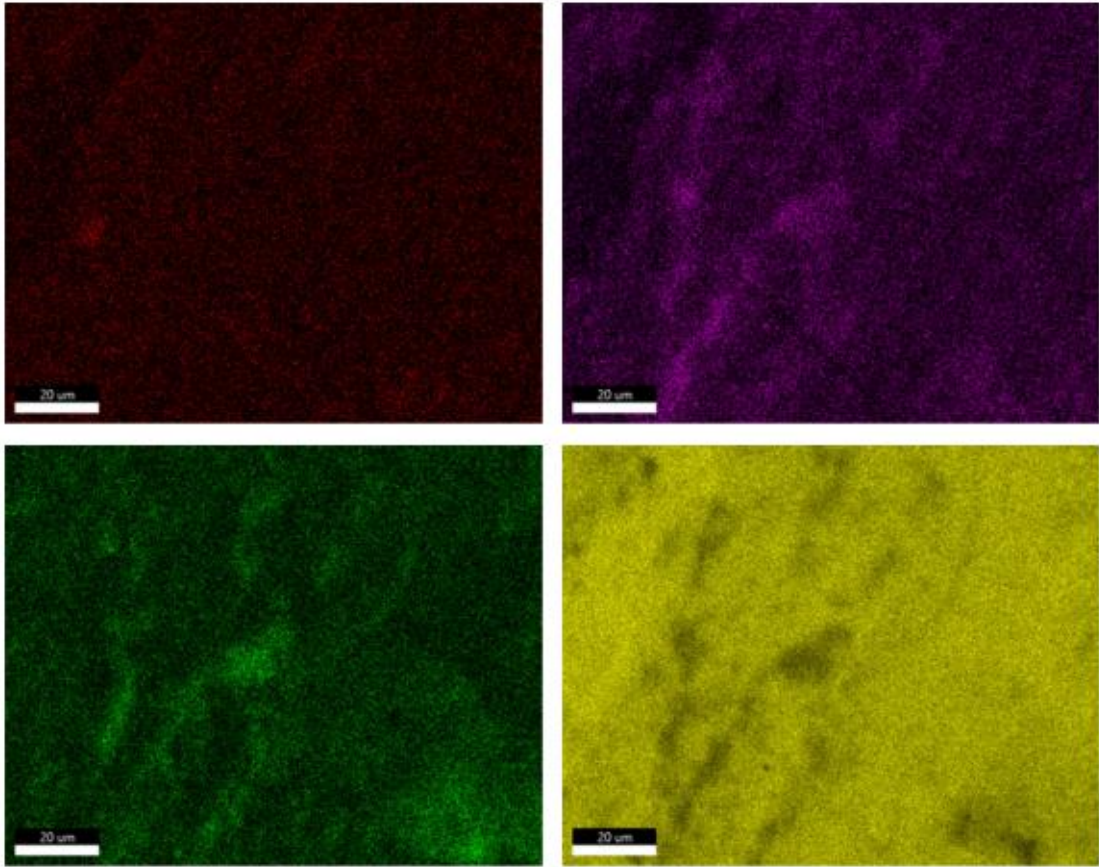
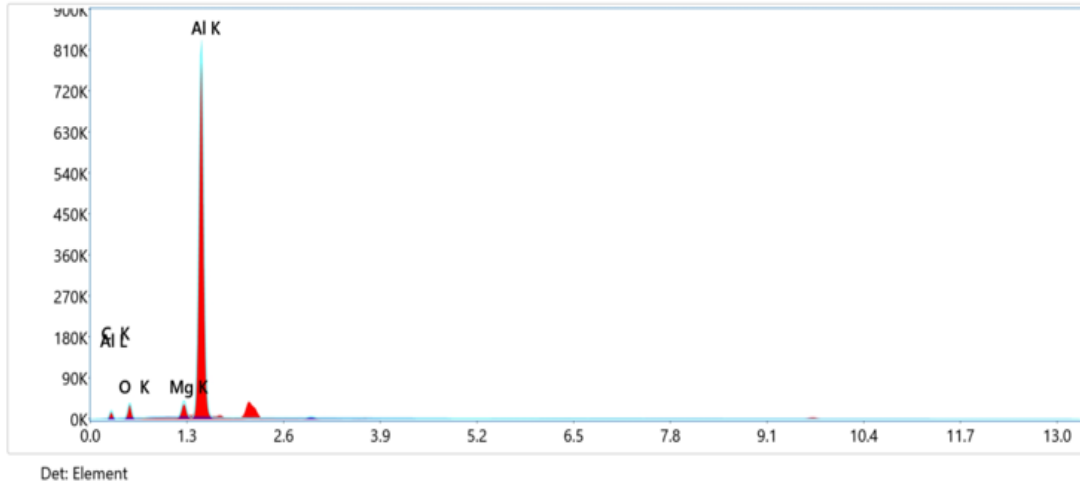


Figure 5.6- 5 EDS mapping of unaged as received sample



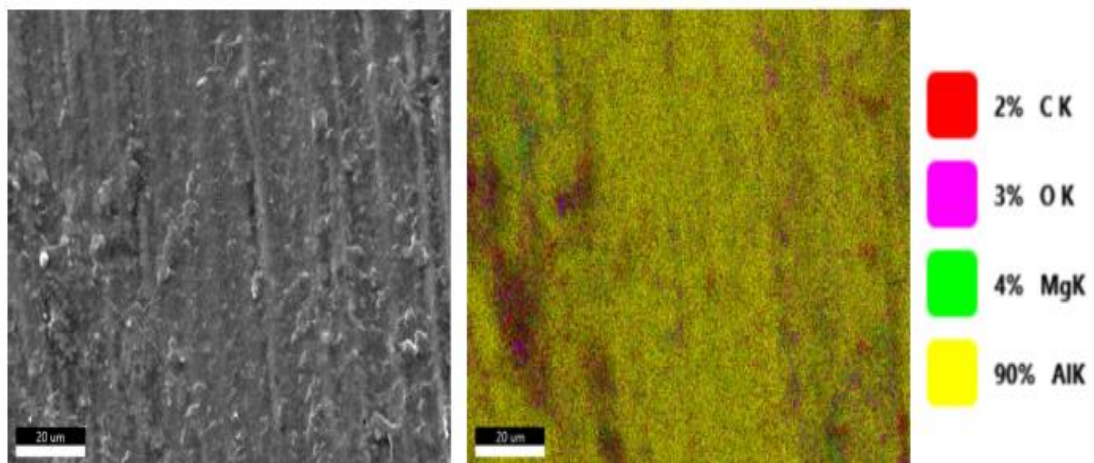
Quant Results

Element	Weight %	MDL	Atomic %	Net Int.	Error %	R	A	F
C K	23.1	0.14	37.8	293.0	11.0	0.9025	0.0305	1.0000
O K	11.5	0.05	14.1	613.0	10.2	0.9133	0.1010	1.0000
Mg K	2.7	0.01	2.2	839.0	5.4	0.9294	0.5921	1.0345
Al K	62.8	0.02	45.9	20006.2	4.2	0.9329	0.6788	1.0015

Figure 5.6- 6 Elemental composition of unaged as received sample

5.6.2.2. Degreased

The EDS mapping of degreased sample also revealed presence of aluminum with small carbon concentrations, figure 5.6-7 and figure 5.6-8. therefore, the failure was mostly adhesive on these degreased surfaces like the as received ones.



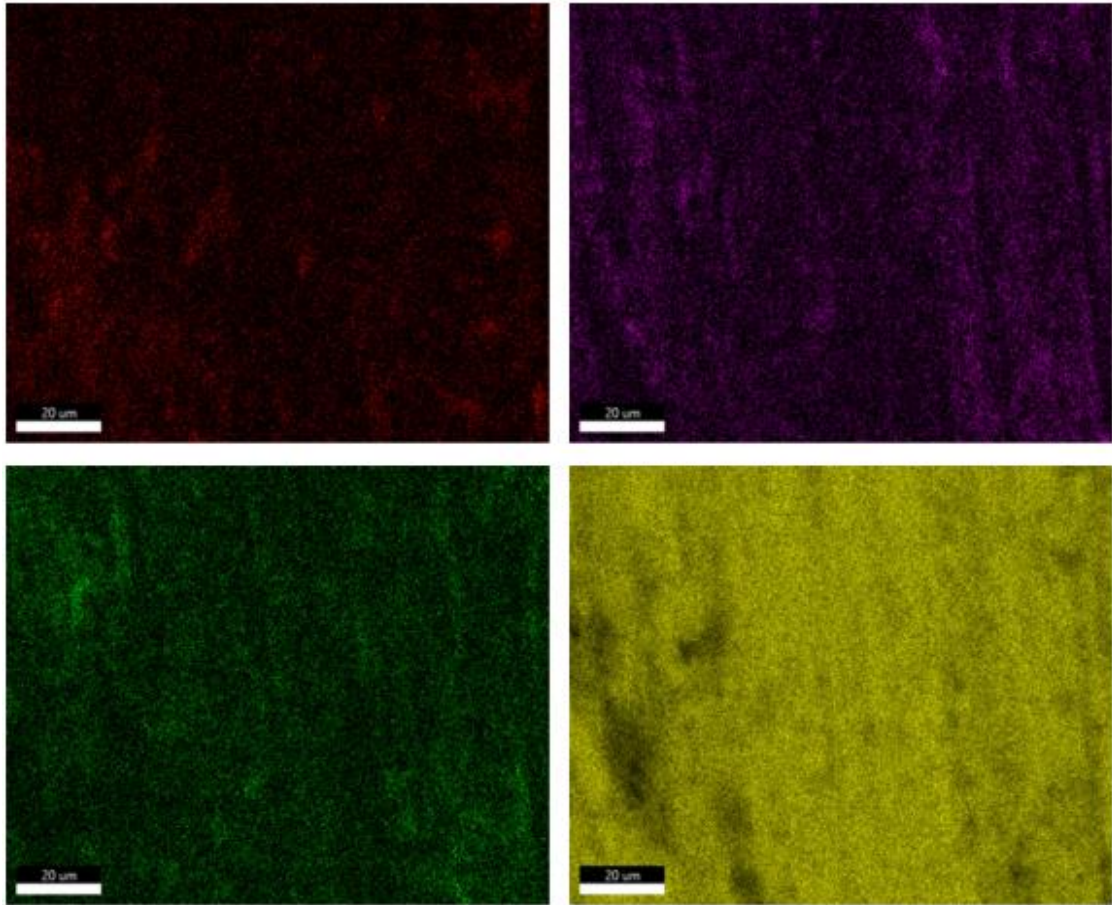
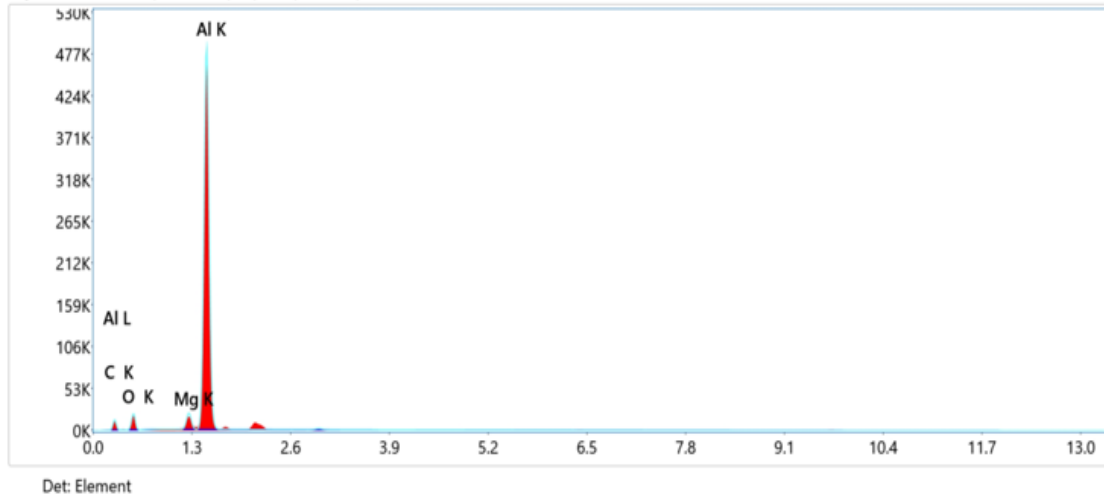


Figure 5.6- 7 EDS mapping of unaged degraded sample



eZAF Quant Result - Analysis Uncertainty: 99.00 %

Element	Weight %	MDL	Atomic %	Net Int.	Error %	R	A	F
C K	26.1	0.15	41.6	346.1	11.0	0.9044	0.0319	1.0000
O K	11.7	0.05	14.0	604.0	10.3	0.9151	0.0978	1.0000
Mg K	2.5	0.01	2.0	761.7	5.5	0.9310	0.5861	1.0333
Al K	59.7	0.02	42.4	18972.1	4.3	0.9345	0.6773	1.0015

Figure 5.6- 8 Elemental composition of unaged degreased sample

5.6.2.3. Grit Blasting with 2cm Distance (GB2)

The greater intensity of carbon at GB2 fracture surfaces indicated the presence of large polymer residue at some regions of these surfaces, Figure 5.6-9. The regions with weak carbon signal showed the absence of polymers at these regions. Since the surface features generated by the grit blasting were not evident at fracture surfaces of these samples, see Figure 5.6-2, there must be some thin layer of the polymer at the areas with weak carbon signals. As the sampling volume of EDX is more therefore thin layer of polymer at some regions was not detected and more sensitive technique like XPS is required. The XPS sampling volume is less, and a thin layer of 3-4 nm can be detected. Therefore, larger carbon signals, Figure 5.6-10, and absence of grit blasted features indicated the presence of polymer residue all over the surface of grit blasted samples. This observation showed polymer into the features of these surfaces and hence the failure was mostly cohesive failure, though pseudo cohesive at some regions.

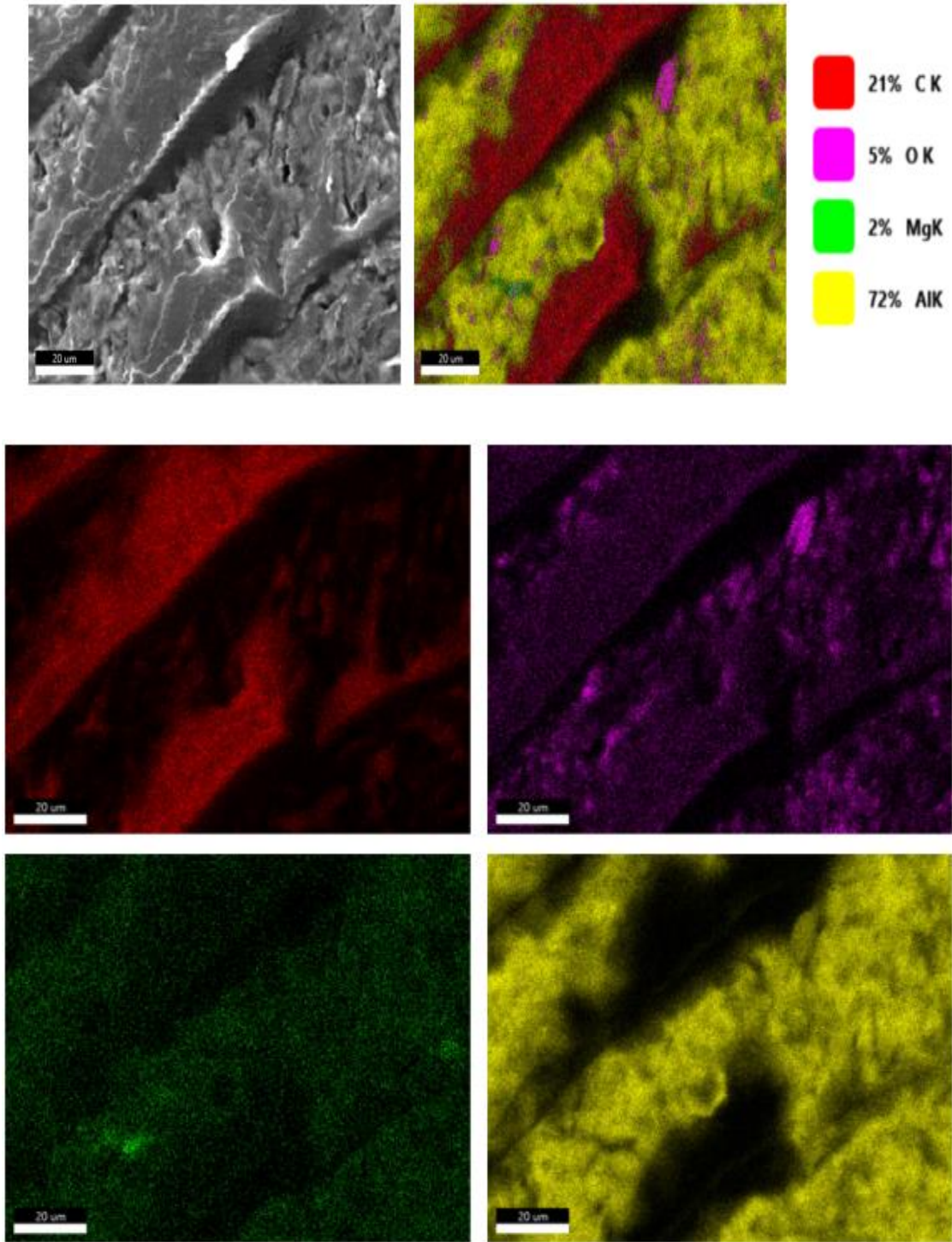
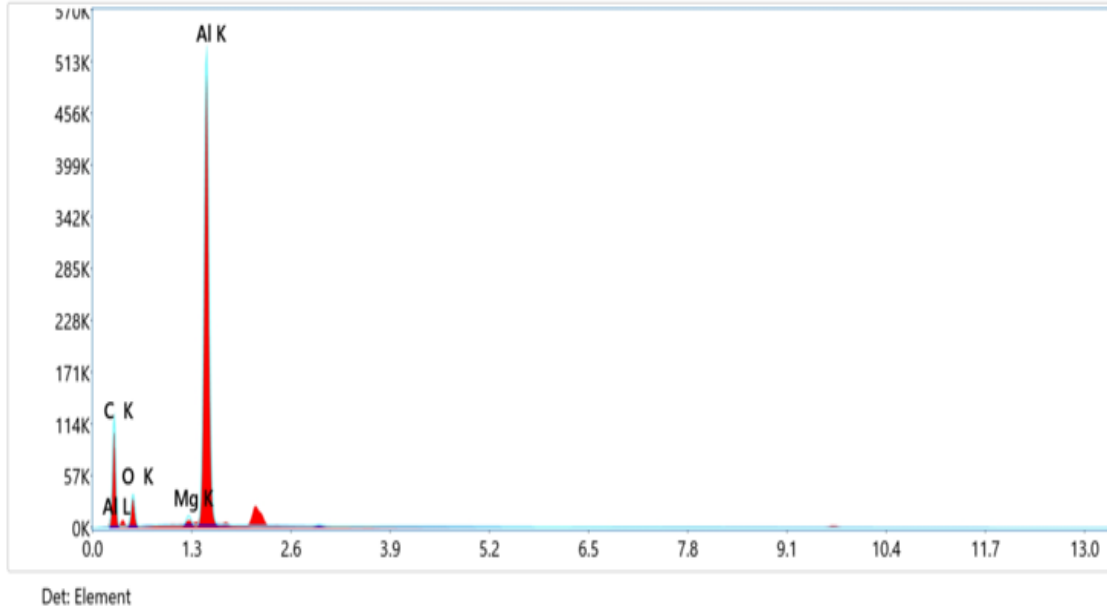


Figure 5.6- 9 EDS mapping of unaged GB2cm sample



eZAF Quant Result - Analysis Uncertainty: 99.00 %

Element	Weight %	MDL	Atomic %	Net Int.	Error %	R	A	F
C K	58.0	0.06	72.1	1993.7	10.4	0.9242	0.0587	1.0000
O K	12.2	0.05	11.4	648.0	10.5	0.9332	0.0716	1.0000
Mg K	0.6	0.01	0.4	240.5	6.2	0.9465	0.5376	1.0197
Al K	29.2	0.01	16.2	12797.6	4.4	0.9493	0.6653	1.0020

Figure 5.6- 10 Elemental composition of unaged GB2cm sample

5.6.2.4. Grit Blasting with 8cm Distance (GB8)

EDX of GB8 fracture surfaces demonstrated a similar behavior like that of GB2 ones, Figure 5.6-11 & Figure 5.6-12. Despite relatively lower carbon concentrations at these GB8 fracture surfaces, the EDX analysis along with the SEM analysis confirmed that failure as mostly cohesive.

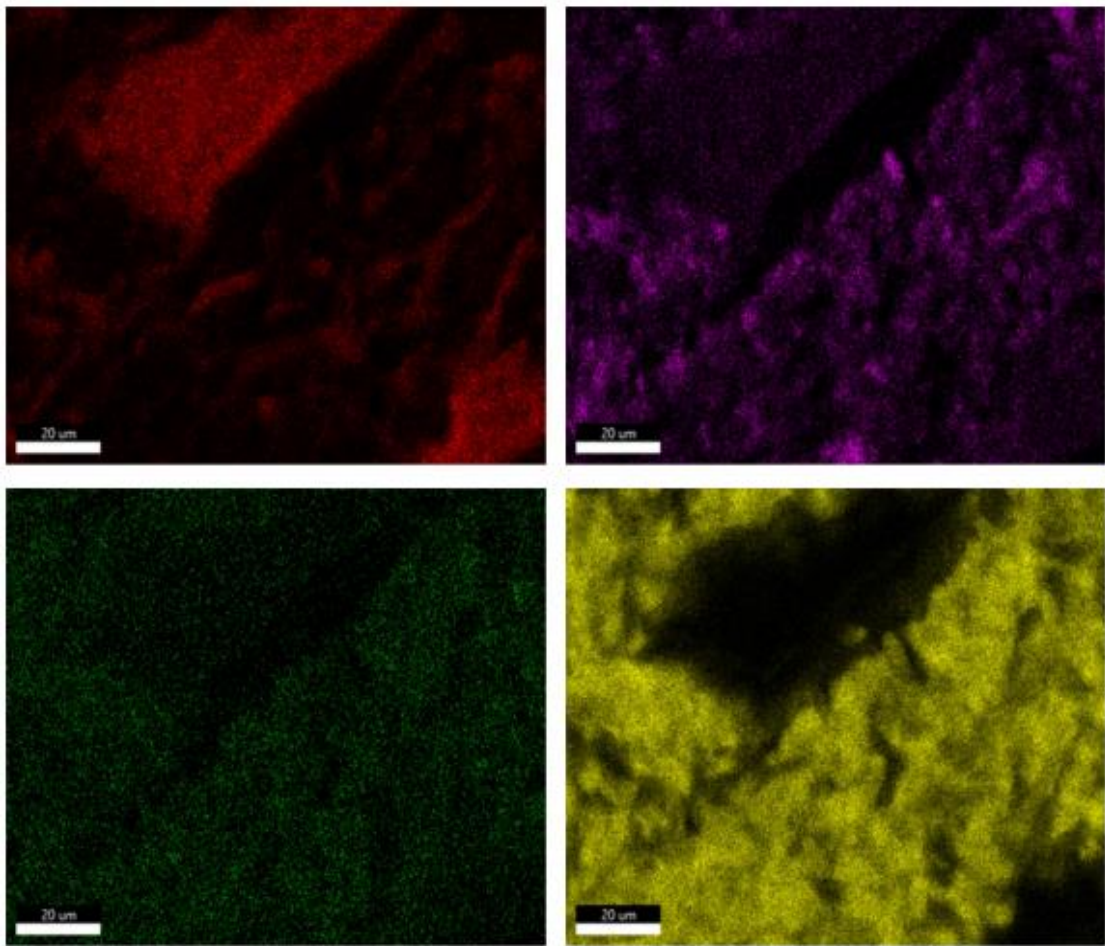
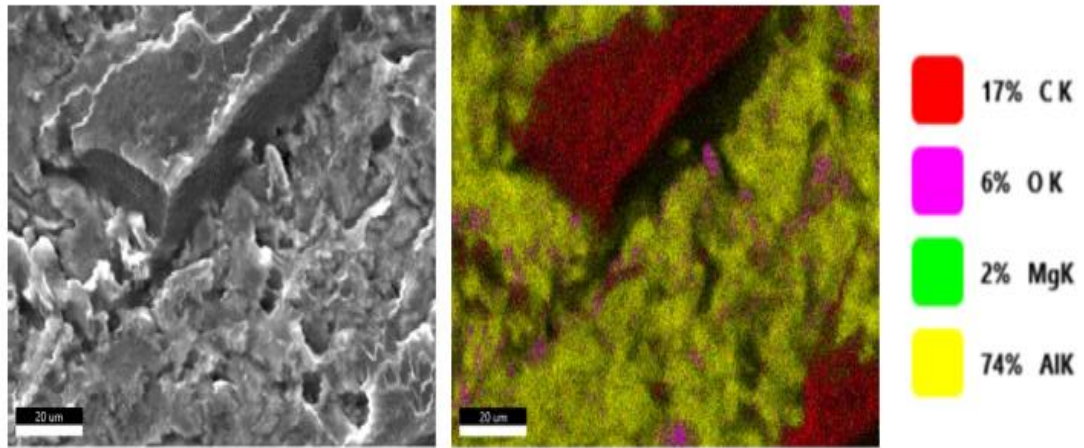
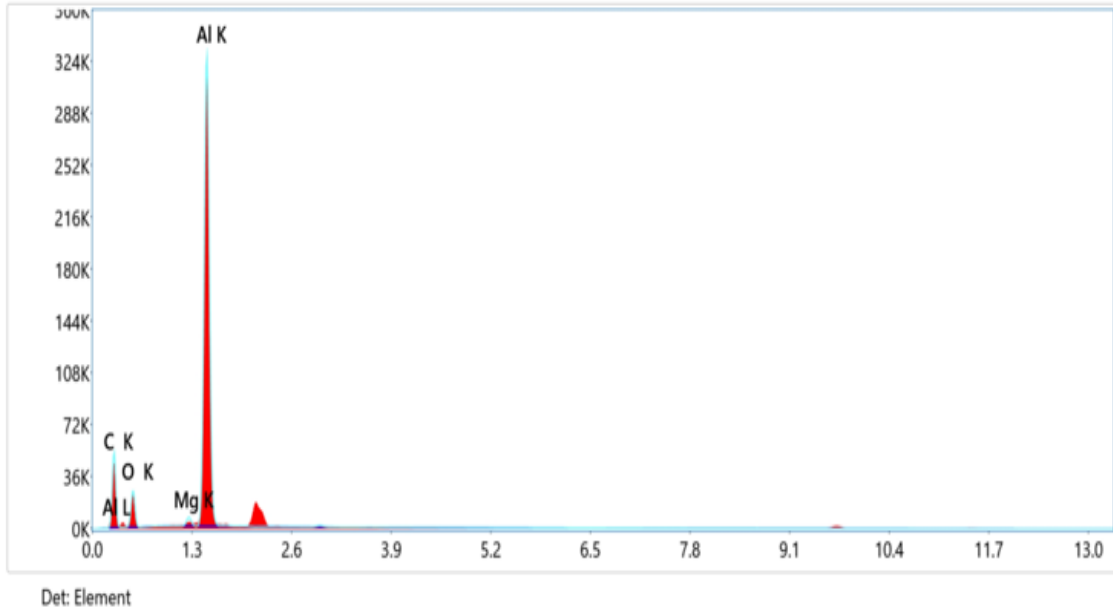


Figure 5.6- 11 EDS mapping of unaged GB 8cm sample



eZAF Quant Result - Analysis Uncertainty: 48.84 %

Element	Weight %	MDL	Atomic %	Net Int.	Error %	R	A	F
C K	51.2	0.09	66.1	1383.7	10.6	0.9211	0.0524	1.0000
O K	14.7	0.06	14.3	745.6	10.4	0.9304	0.0773	1.0000
Mg K	0.7	0.01	0.4	223.9	6.6	0.9441	0.5347	1.0214
Al K	33.5	0.01	19.2	12845.2	4.4	0.9471	0.6618	1.0019

Figure 5.6- 12 Elemental composition of unaged GB 8cm sample

5.7. Fracture analysis: aged samples

5.7.1. Morphological study

5.7.1.1. As Received

SE image of as received aged sample showed no polymer residues at the fracture surface, Figure 5.7-1. SEM images revealed hydration of the surfaces during hydrothermal aging manifesting very poor hydration resistance of as received surfaces. This hydration resulted in complete delamination of the polymer from the substrate surfaces resulting in zero lap shear strengths.

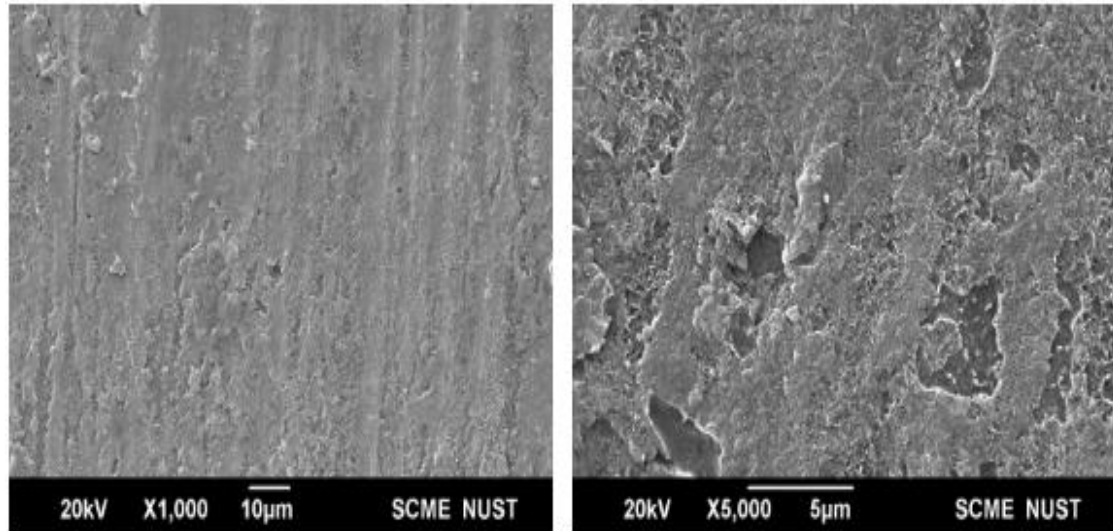


Figure 5.7- 1 Fracture surface of aged As Received sample

5.7.1.2. Degreased

SE image of aged fracture surfaces also confirmed hydration of the degreased surface during hydrothermal aging, Figure 5.7-2. Therefore, the failure was completely adhesion one with no lap shear strengths.

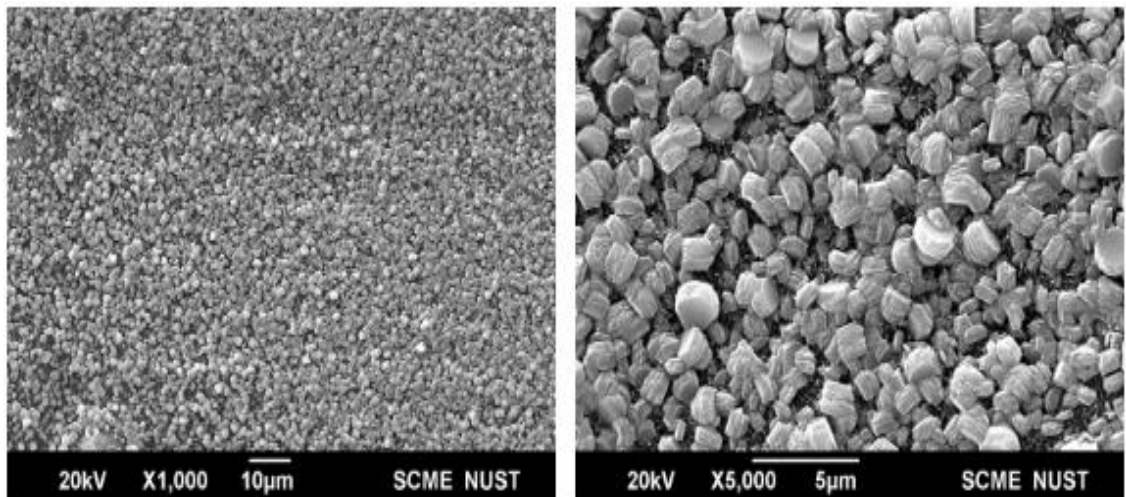


Figure 5.7- 2 Fracture surface of aged Degreased sample

5.7.1.3. Grit Blasting with 2cm Distance (GB2)

The loci of failure were at the oxide/hydroxide-polymer interfaces for aged GB2 samples Figure 5.7-3. Apparently, there were no large polymer residues at the fracture surfaces showing mostly adhesive failure at these surfaces. However, there were no indications of severe hydration of these surfaces compared to the as received or degreased ones. This observation indicated the better hydration resistance of these surfaces.

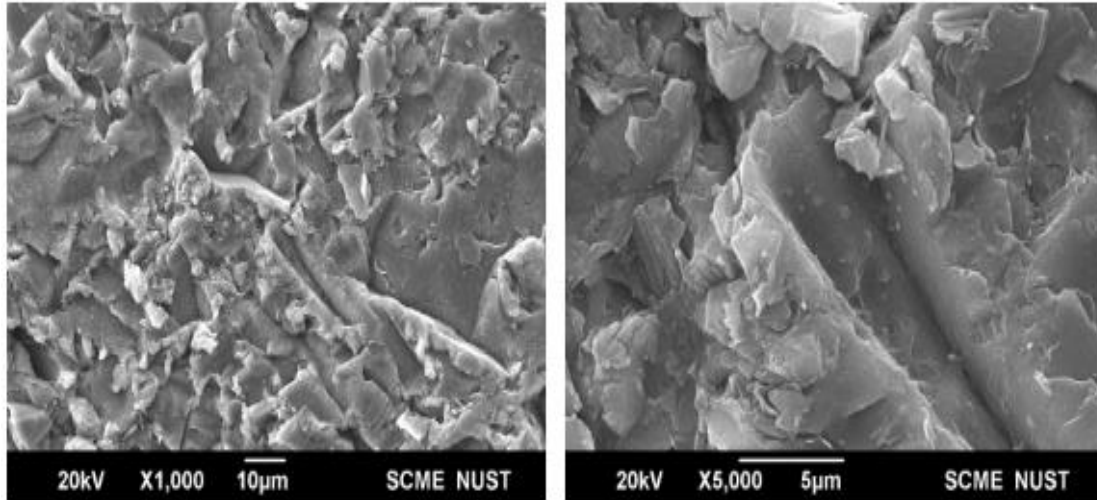


Figure 5.7- 3 Fracture surface of aged GB2cm sample

5.7.1.4. Grit Blasting with 8cm Distance (GB8)

The loci of failure for aged GB8 samples were also at the oxide/hydroxide-polymer interfaces, Figure 5.7-4. Detached oxide (possibly hydrated one) is also present at the fracture surface of aged PA6 bonded joints treated with GB8cm.

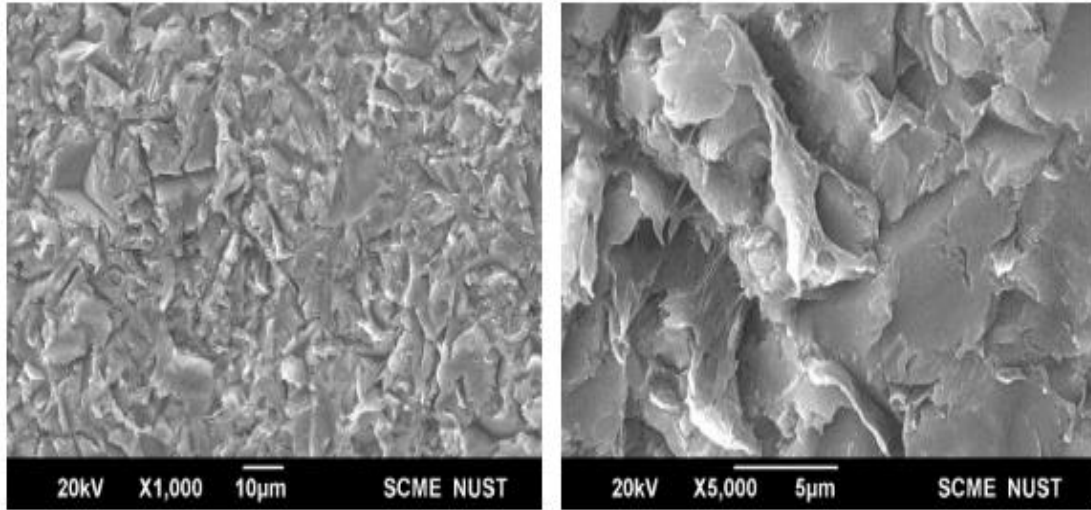
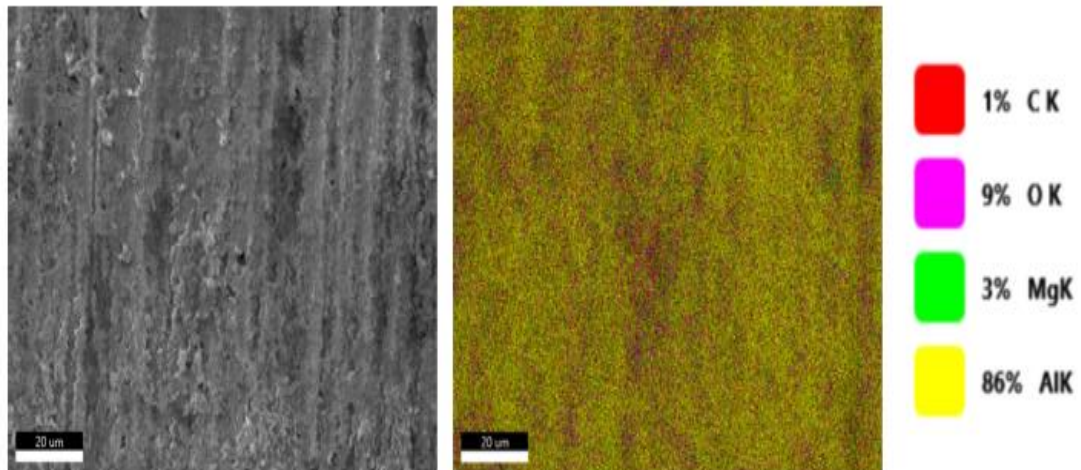


Figure 5.7- 4 Fracture surface of aged GB 8cm sample

5.7.2. Compositional study

5.7.2.1. As Received

The oxygen and aluminum signal are intense in AR fracture samples, figure 5.7-5 & figure 5.7-6. The more oxygen content indicates that there were possibly thick oxides or hydroxide layers present as these samples after subjected to aging. The absence of polymer indicated complete adhesive failure.



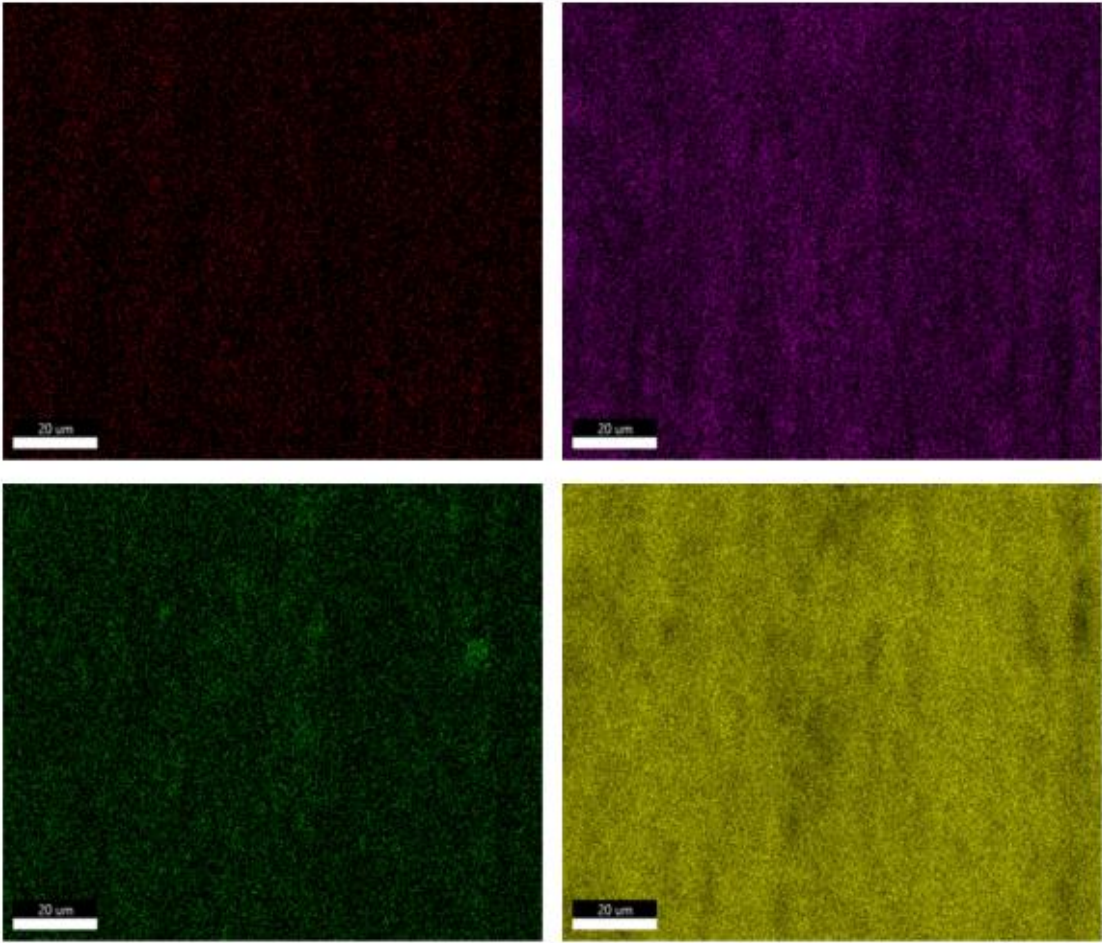
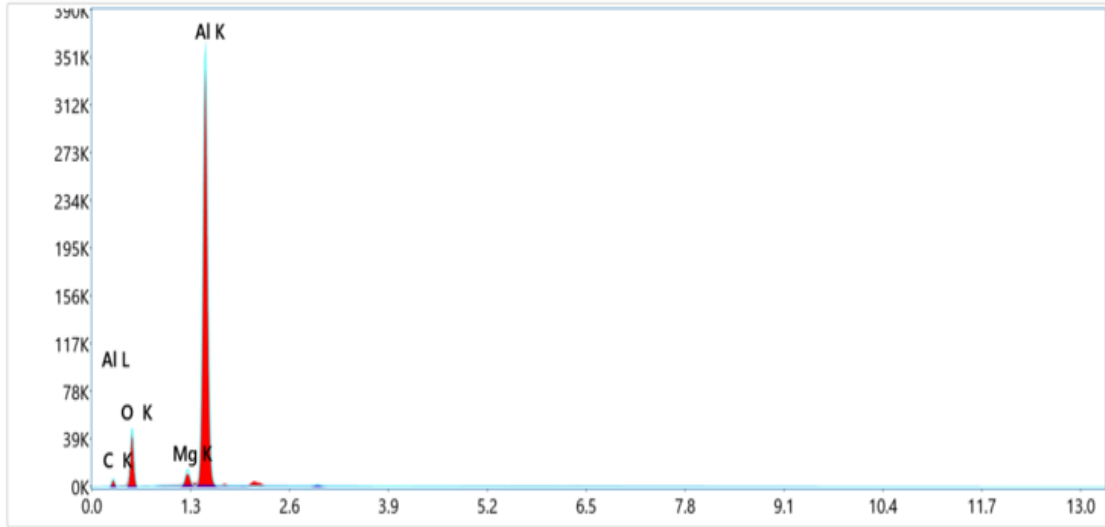


Figure 5.7- 5 EDS mapping of aged as received sample



eZAF Quant Result - Analysis Uncertainty: 99.00 %

Element	Weight %	MDL	Atomic %	Net Int.	Error %	R	A	F
C K	15.3	0.13	25.1	215.1	11.3	0.9039	0.0326	1.0000
O K	25.9	0.03	31.8	1773.4	9.8	0.9146	0.1253	1.0000
Mg K	2.2	0.01	1.8	627.6	6.2	0.9305	0.5317	1.0284
Al K	56.6	0.01	41.3	17510.1	4.7	0.9340	0.6378	1.0015

Figure 5.7- 6 Elemental composition of aged as received sample

5.7.2.2. Degreased

The EDX analysis along with the SEM studies of degreased and aged samples also confirmed the hydration of these surfaces during aging, figure 5.7-7 & figure 5.7-8.

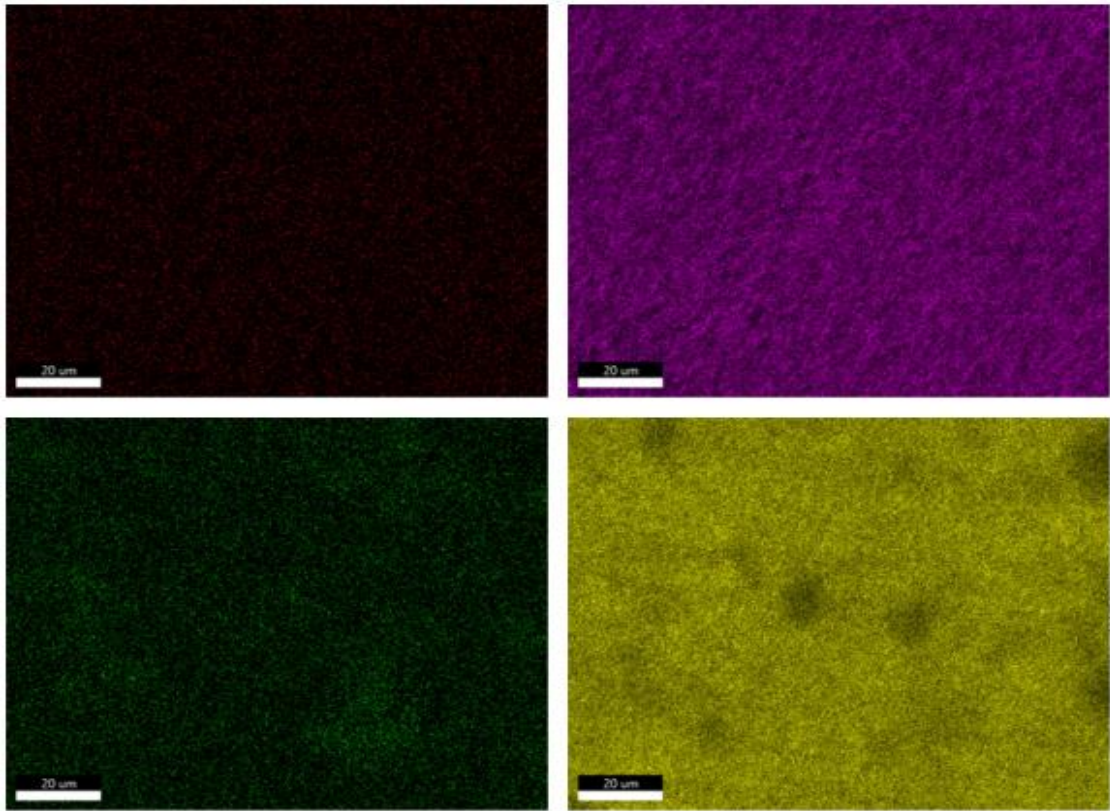
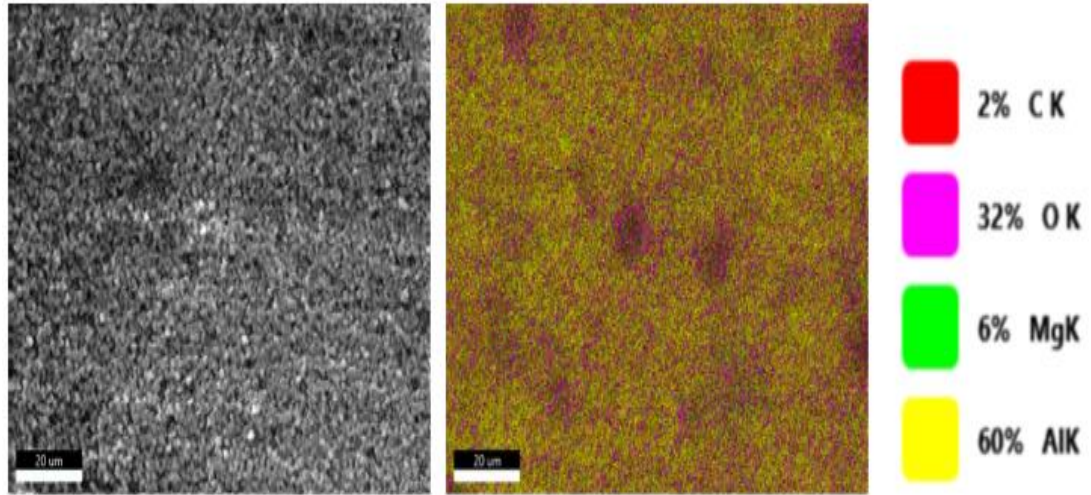
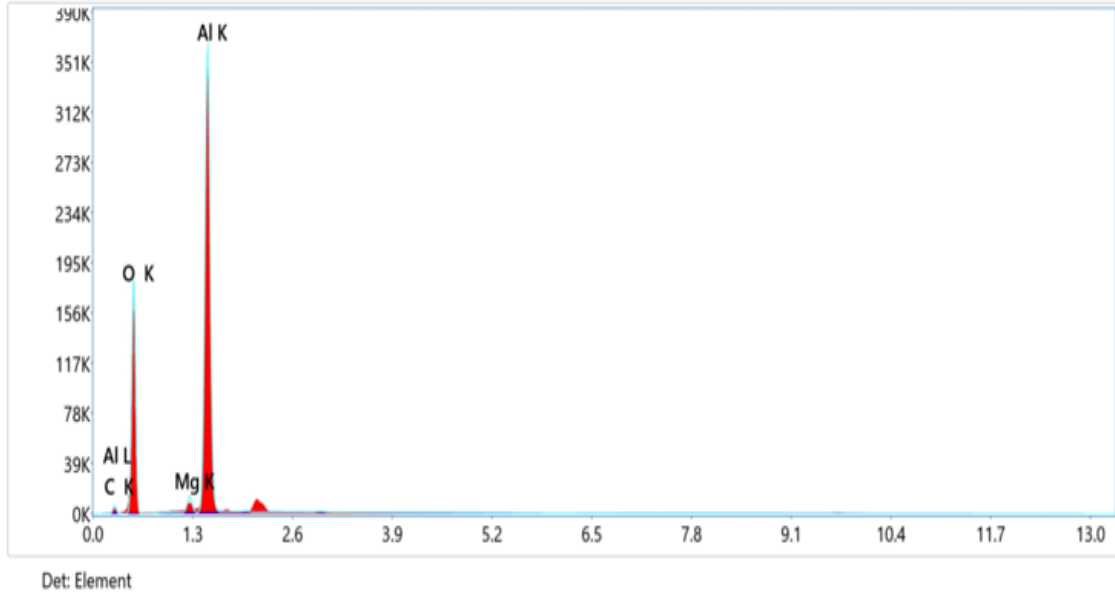


Figure 5.7- 7 EDS mapping of aged, degreased sample



eZAF Quant Result - Analysis Uncertainty: 39.27 %

Element	Weight %	MDL	Atomic %	Net Int.	Error %	R	A	F
C K	8.0	0.09	12.5	133.5	11.3	0.9087	0.0391	1.0000
O K	47.6	0.01	56.2	4542.6	9.3	0.9190	0.1755	1.0000
Mg K	1.7	0.01	1.3	400.0	7.0	0.9343	0.4519	1.0192
Al K	42.8	0.01	30.0	11882.1	5.3	0.9377	0.5763	1.0017

Figure 5.7- 8 Elemental composition of aged, degreased sample

5.7.2.3. Grit Blasting with 2cm Distance (GB2)

Though SEM analysis of fracture surface of GB2 confirmed adhesive failure, however, the EDX of these samples showed that polymer residues were present because carbon signal were detected at these surfaces, figure 5.7-9 & figure 5.7-10. Therefore, GB2 did not show complete adhesive failure along with no apparent hydration of the aged surfaces.

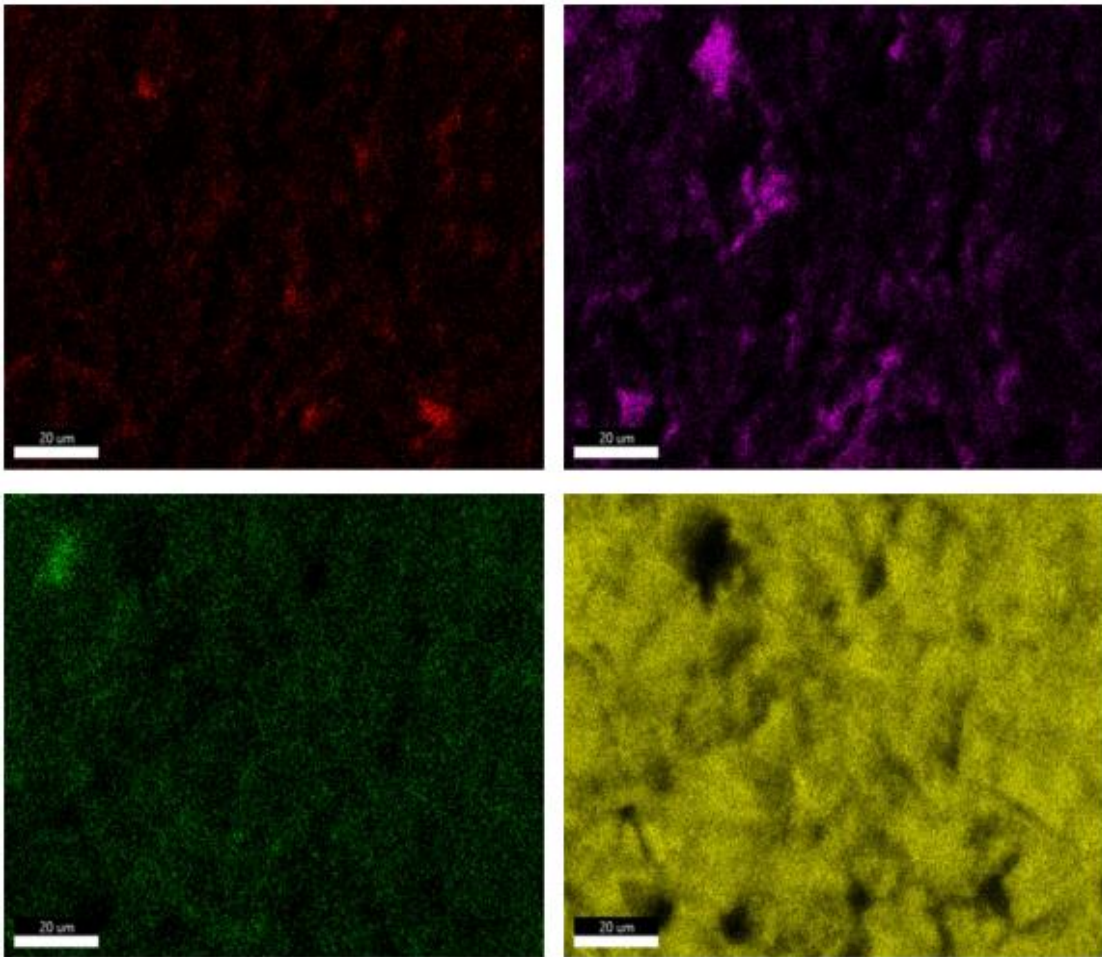
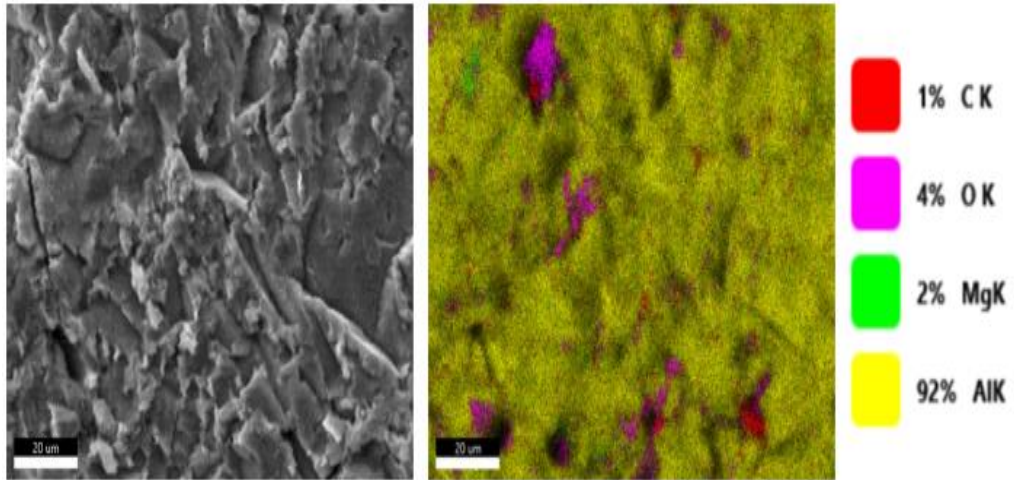
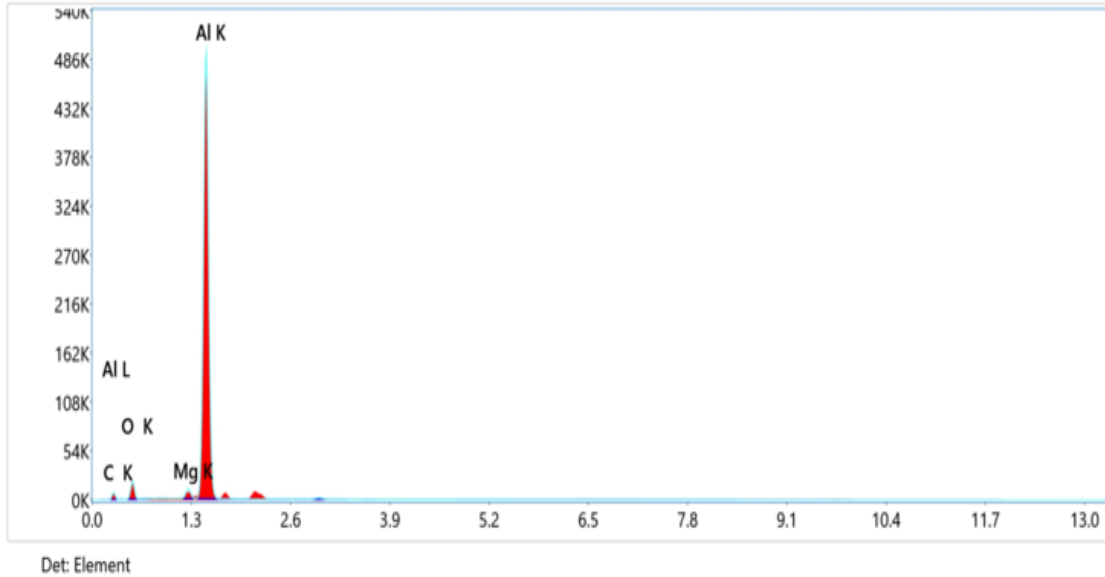


Figure 5.7- 9 EDS mapping of aged GB2cm sample



eZAF Quant Result - Analysis Uncertainty: 39.27 %

Element	Weight %	MDL	Atomic %	Net Int.	Error %	R	A	F
C K	19.5	0.18	33.1	208.7	11.3	0.9004	0.0291	1.0000
O K	11.8	0.06	15.1	580.0	10.2	0.9113	0.1051	1.0000
Mg K	1.5	0.02	1.3	415.8	5.7	0.9277	0.5949	1.0385
Al K	67.1	0.02	50.6	19310.9	4.1	0.9313	0.6962	1.0015

Figure 5.7- 10 Elemental composition of aged GB2cm sample

5.7.2.4. Grit Blasting with 8cm Distance (GB8)

The behavior of GB8 fracture surfaces was quite like the GB2 ones, figure 5.7-11 & figure 5.7-12. Therefore, GB surfaces performed better compared to the degreased or as received ones, under aged and unaged conditions.

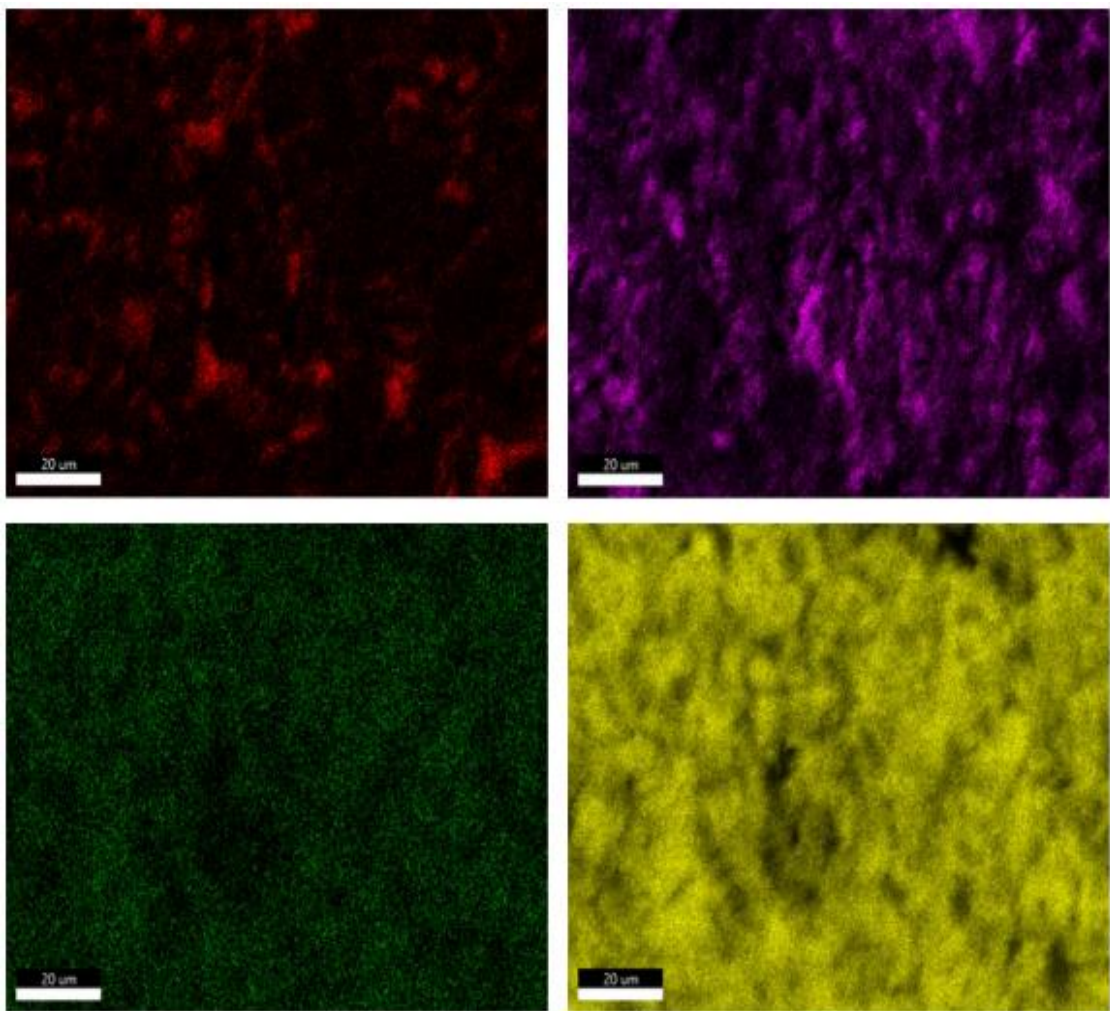
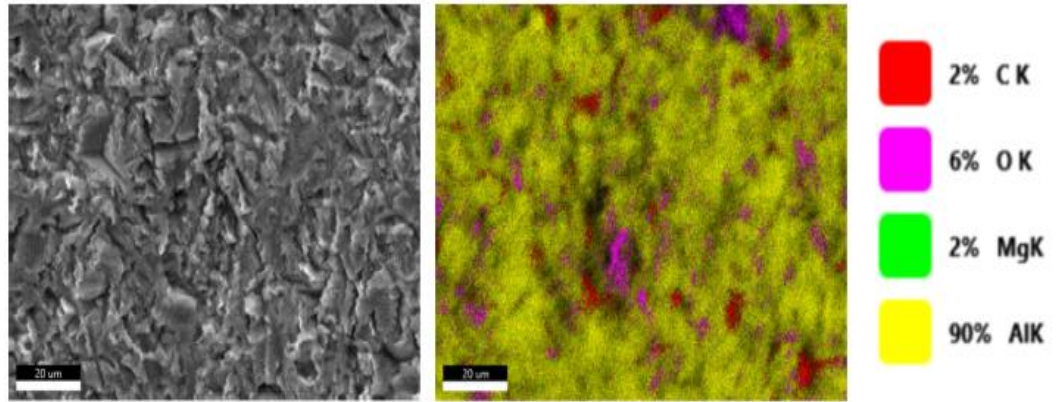
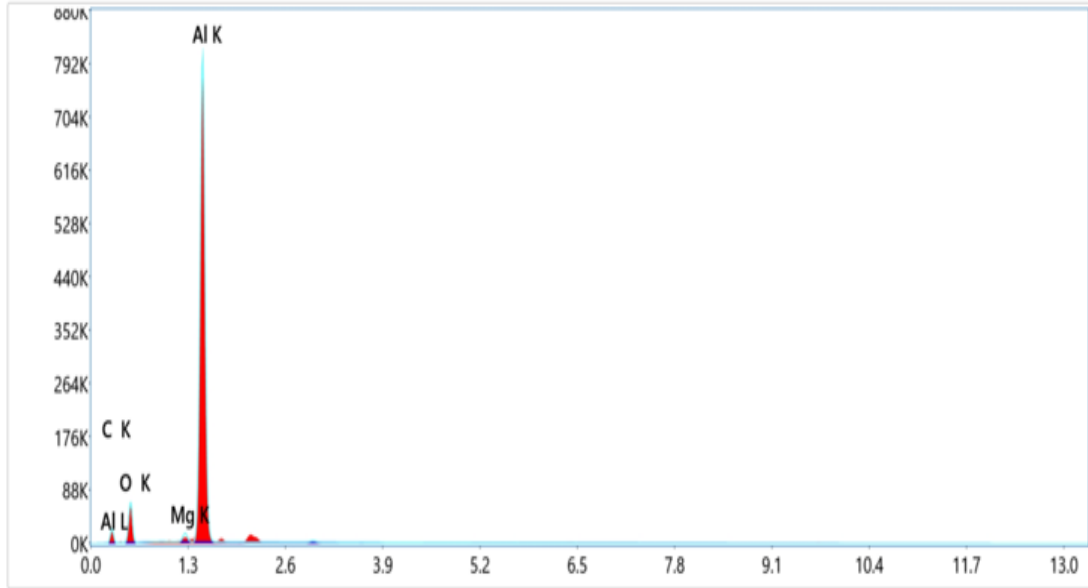


Figure 5.7- 11 EDS mapping of aged GB 8cm sample



Det: Element

eZAF Quant Result - Analysis Uncertainty: 45.10 %

Element	Weight %	MDL	Atomic %	Net Int.	Error %	R	A	F
C K	23.9	0.10	37.5	339.3	10.9	0.9063	0.0339	1.0000
O K	19.5	0.04	22.9	1100.1	10.0	0.9169	0.1062	1.0000
Mg K	1.0	0.01	0.8	286.7	6.1	0.9325	0.5494	1.0312
Al K	55.6	0.01	38.8	17517.2	4.4	0.9359	0.6672	1.0016

Figure 5.7- 12 Elemental composition of aged GB 8cm sample

Conclusions

Surface pretreatment by grit blasting and anodizing can effectively replace as received and degreased sample of the alloy AA-6061. Solvent degreasing surface pretreatment only removes some of the loose surface contaminants, which can help with initial adhesion but is not helpful for the long-term durability of adhesively bonded joints in severe environments. The Grit Blasted surface shows good roughness Ra value of 14 μm and 15.1 μm as compared to degreased samples which was 0.52 μm . The grit blasted sample GB2, and anodized sample show good lap shear strength of 19.16 MPa and 15.71 MPa. Fracture analysis of the shows that the polymer residue is present on treated surface of grit blasted samples and the features are less means polymer is infiltrated into the reentrant geometries and hence shows better lap shear strength as compared to as received and degreased samples. High surface adhesion and durability was due to mechanical interlocking along with other interactions such as chemical interactions. Although anodized samples show high strength, but the durability of anodized samples was poor but usually they show good durability but, in our case, it shows poor aging resistance further investigation are required to solve this anomaly.

References

- [1] A. Kinloch, M. Little, and J. J. A. m. Watts, "The role of the interphase in the environmental failure of adhesive joints," vol. 48, no. 18-19, pp. 4543-4553, (2000).
- [2] A. J. J. o. m. s. Baldan, "Adhesively-bonded joints and repairs in metallic alloys, polymers and composite materials: Adhesives, adhesion theories and surface pretreatment," vol. 39, no. 1, pp. 1-49, (2004).
- [3] A. J. J. o. M. S. Baldan, "Adhesively-bonded joints in metallic alloys, polymers and composite materials: Mechanical and environmental durability performance," vol. 39, no. 15, pp. 4729-4797, (2004).
- [4] F. L. Palmieri *et al.*, "Laser ablative surface treatment for enhanced bonding of Ti-6Al-4V alloy," vol. 5, no. 4, pp. 1254-1261, (2013).
- [5] E. Andrews and N. J. J. o. M. S. King, "Adhesion of epoxy resins to metals," vol. 11, no. 11, pp. 2004-2014, (1976).
- [6] M. Davis, D. J. I. j. o. a. Bond, and adhesives, "Principles and practices of adhesive bonded structural joints and repairs," vol. 19, no. 2-3, pp. 91-105, (1999).
- [7] J. Evans and D. Packham, "Adhesion of polyethylene to metals: The role of surface topography," (1979).
- [8] M. Irfan, B. D. Zander, and G. Requena, "Development and characterisation of surface pretreatments of aluminium AA6082-T6 for adhesion applications," (2020).
- [9] F. M. J. J. o. A. S. Fowkes and Technology, "Role of acid-base interfacial bonding in adhesion," vol. 1, no. 1, pp. 7-27, (1987).
- [10] R. Frenzel *et al.*, "Polyelectrolytes to promote adhesive bonds of laser-structured aluminium," vol. 61, pp. 35-45, (2015).
- [11] R. Gledhill and A. J. T. j. o. a. Kinloch, "Environmental failure of structural adhesive joints," vol. 6, no. 4, pp. 315-330, (1974).
- [12] R. J. Davies, "The durability of an adhesively bonded aluminium alloy," (1990).
- [13] J. Zhang, X. Zhao, Y. Zuo, J. Xiong, X. J. J. o. M. S. Zhang, and Technology, "Effect of surface pretreatment on adhesive properties of aluminum alloys," vol. 24, no. 2, pp. 236-240, (2008).
- [14] "<Baldan(2004)_Article_Adhesively-bondedJointsAndRepa.pdf>."
- [15] D. A. Dillard, *Advances in structural adhesive bonding*. Elsevier, (2010).
- [16] F. M. Dos Santos *et al.*, "The Effect of Aluminium Surface Treatments on the Bonding Properties of Silica-Modified Epoxy Adhesive Joints: A Statistical Approach," vol. 10, pp. 17-26, (2021).

- [17] S. Y. Park, W. J. Choi, H. S. Choi, H. Kwon, and S. H. J. T. J. o. A. Kim, "Recent trends in surface treatment technologies for airframe adhesive bonding processing: a review (1995–2008)," vol. 86, no. 2, pp. 192-221, (2010).
- [18] S. N. E. Sumaiya, "Effect of surface treatments on interfacial strength and durability of metal-polymer composite bond," (2016).
- [19] S. Budhe, A. Ghumatkar, N. Birajdar, and M. J. A. A. S. Banea, "Effect of surface roughness using different adherend materials on the adhesive bond strength," vol. 3, no. 1, pp. 1-10, (2015).
- [20] J. D. Minford, *Handbook of aluminum bonding technology and data*. CRC Press, (1993).
- [21] F. L. Palmieri, M. A. Belcher, C. J. Wohl, K. Y. Blohowiak, J. W. J. I. J. o. A. Connell, and Adhesives, "Laser ablation surface preparation for adhesive bonding of carbon fiber reinforced epoxy composites," vol. 68, pp. 95-101, (2016).
- [22] R. Rechner, I. Jansen, E. J. I. J. o. A. Beyer, and Adhesives, "Influence on the strength and aging resistance of aluminium joints by laser pre-treatment and surface modification," vol. 30, no. 7, pp. 595-601, (2010).
- [23] A. A. Roche, M. Aufray, and J. J. T. J. o. A. Bouchet, "The role of the residual stresses of the epoxy-aluminum interphase on the interfacial fracture toughness," vol. 82, no. 9, pp. 867-886, (2006).
- [24] N. M. Zain, S. H. Ahmad, E. S. J. I. J. o. A. Ali, and Adhesives, "Effect of surface treatments on the durability of green polyurethane adhesive bonded aluminium alloy," vol. 55, pp. 43-55, (2014).
- [25] K.-T. Wan, A. Di Prima, L. Ye, and Y.-W. J. J. o. m. s. Mai, "Adhesion of nylon-6 on surface treated aluminium substrates," vol. 31, no. 8, pp. 2109-2116, (1996).
- [26] T. Sinmazçelik, E. Avcu, M. Ö. Bora, O. J. M. Çoban, and Design, "A review: Fibre metal laminates, background, bonding types and applied test methods," vol. 32, no. 7, pp. 3671-3685, (2011).
- [27] A. Harris, A. J. I. j. o. a. Beevers, and adhesives, "The effects of grit-blasting on surface properties for adhesion," vol. 19, no. 6, pp. 445-452, (1999).
- [28] A. Rudawska, M. Wahab, and M. Müller, "Strength of Epoxy-Bonded Aluminium Alloy Joints after Sandblasting," *Advances in Science and Technology Research Journal*, vol. 16, no. 2, pp. 262-279, (2022).
- [29] S. G. Prolongo and A. Ureña, "Effect of surface pre-treatment on the adhesive strength of epoxy–aluminium joints," *International Journal of Adhesion and Adhesives*, vol. 29, no. 1, pp. 23-31, (2009).
- [30] M. Paz Martínez-Viademonte, S. T. Abrahami, T. Hack, M. Burchardt, and H. J. C. Terryn, "A review on anodizing of aerospace aluminum alloys for corrosion protection," vol. 10, no. 11, p. 1106, (2020).

- [31] J.-s. Zhang, X.-h. Zhao, Y. Zuo, J.-p. J. S. Xiong, and C. Technology, "The bonding strength and corrosion resistance of aluminum alloy by anodizing treatment in a phosphoric acid modified boric acid/sulfuric acid bath," vol. 202, no. 14, pp. 3149-3156, (2008).
- [32] A. Spaggiari and E. Dragoni, "Effect of Mechanical Surface Treatment on the Static Strength of Adhesive Lap Joints," *The Journal of Adhesion*, vol. 89, no. 9, pp. 677-696, (2013).
- [33] S. G. Prolongo, G. Rosario, and A. Ureña, "Study of the effect of substrate roughness on adhesive joints by SEM image analysis," *Journal of Adhesion Science and Technology*, vol. 20, no. 5, pp. 457-470, (2006).
- [34] N. Saleema and D. Gallant, "Atmospheric pressure plasma oxidation of AA6061-T6 aluminum alloy surface for strong and durable adhesive bonding applications," *Applied Surface Science*, vol. 282, pp. 98-104, (2013).
- [35] S. S. Golru, M. M. Attar, and B. Ramezanzadeh, "Effects of different surface cleaning procedures on the superficial morphology and the adhesive strength of epoxy coating on aluminium alloy 1050," *Progress in Organic Coatings*, vol. 87, pp. 52-60, (2015).
- [36] T. S. Williams, H. Yu, and R. F. Hicks, "Atmospheric pressure plasma activation as a surface pre-treatment for the adhesive bonding of aluminum 2024," *Journal of Adhesion Science and Technology*, vol. 28, no. 7, pp. 653-674, (2013).
- [37] Y. Xu, H. Li, Y. Shen, S. Liu, W. Wang, and J. Tao, "Improvement of adhesion performance between aluminum alloy sheet and epoxy based on anodizing technique," *International Journal of Adhesion and Adhesives*, vol. 70, pp. 74-80, (2016).
- [38] J. Venables, D. McNamara, J. Chen, T. Sun, and R. J. A. o. S. S. Hopping, "Oxide morphologies on aluminum prepared for adhesive bonding," vol. 3, no. 1, pp. 88-98, (1979).
- [39] L. Goglio and M. Rezaei, "Effect of Different Substrate Pre-Treatments on the Resistance of Aluminum Joints to Moist Environments," *The Journal of Adhesion*, vol. 89, no. 10, pp. 769-784, (2013).
- [40] L. Dong, Y. Li, M. Huang, X. Hu, Z. Qu, and Y. Lu, "Effect of anodizing surface morphology on the adhesion performance of 6061 aluminum alloy," *International Journal of Adhesion and Adhesives*, vol. 113, (2022).
- [41] G. Critchlow, D. J. I. j. o. a. Brewis, and adhesives, "Influence of surface macroroughness on the durability of epoxide-aluminium joints," vol. 15, no. 3, pp. 173-176, (1995).
- [42] A. Bjørgum, F. Lapique, J. Walmsley, K. J. I. j. o. a. Redford, and adhesives, "Anodising as pre-treatment for structural bonding," vol. 23, no. 5, pp. 401-412, (2003).

- [43] J. Weiss *et al.*, "Ageing mechanisms of polyurethane adhesive/steel interfaces," vol. 70, pp. 167-175, (2016).